PHYSICAL REVIEW E **95**, 063302 (2017)

Asymptotic modeling of transport phenomena at the interface between a fluid and a porous layer: Jump conditions

Philippe Angot,[1] Benoît Goyeau,[2,*] and J. Alberto Ochoa-Tapia[3]

[1]*Aix-Marseille Université, Institut de Mathématiques de Marseille, UMR-CNRS 7373, Centrale Marseille, 39 rue F. Joliot-Curie, 13453 Marseille cedex 13, France*

[2]*EM2C, UPR-CNRS 288, Ecole CentraleSupélec, Grande Voie des Vignes, 92295 Châtenay-Malabry, France*

[3]*Departamento de Ingeniería de Procesos e Hidráulica, Universidad Autónoma Metropolitana-Iztapalapa, Mexico 09340 D.F., Mexico*

(Received 25 December 2016; published 8 June 2017)

We develop asymptotic modeling for two- or three-dimensional viscous fluid flow and convective transfer at the interface between a fluid and a porous layer. The asymptotic model is based on the fact that the thickness d of the interfacial transition region $\Omega_{\rm fp}$ of the one-domain representation is very small compared to the macroscopic length scale L. The analysis leads to an equivalent two-domain representation where transport phenomena in the transition layer of the one-domain approach are represented by algebraic jump boundary conditions at a fictive dividing interface Σ between the homogeneous fluid and porous regions. These jump conditions are thus stated up to first-order in $O(d/L)$ with $d/L \ll 1$. The originality and relevance of this asymptotic model lies in its general and multidimensional character. Indeed, it is shown that all the jump interface conditions derived for the commonly used 1D-shear flow are recovered by taking the tangential component of the asymptotic model. In that case, the comparison between the present model and the different models available in the literature gives explicit expressions of the effective jump coefficients and their associated scaling. In addition for multi-dimensional flows, the general asymptotic model yields the different components of the jump conditions including a new specific equation for the cross-flow pressure jump on Σ.

DOI: 10.1103/PhysRevE.95.063302

I. INTRODUCTION

Due to its interest for industrial or natural configurations, transport phenomena between a fluid and a porous layer have been the subject of intense research activity from the pioneering study by Beavers and Joseph [1], where a Poiseuille flow over a permeable medium was considered. Most theoretical and experimental studies concerning momentum transport have used the same configuration in order to characterize velocity fields at the different scales of the interfacial region. Experiments mainly focused at the pore scale, where new measurement techniques, such as particle image velocimetry (PIV), have provided velocity profiles and estimation of the size of the interfacial layer for granular and fibrous porous media [2–8]. Similarly, the development of computational resources allowed pore-scale numerical simulations (DNS, lattice-Boltzmann), leading to local representations in the interfacial region [9–11].

Despite the accuracy of those local (microscopic) descriptions, the complexity of real partially porous systems involving very different characteristic length scales often requires an average representation of transport phenomena. Such a macroscopic modeling is obtained by upscaling the pore-scale equations giving rise to two average modeling approaches: the single- and the two-domain models. The single-domain (or one-domain approach), initially introduced in Ref. [12], considers the plain fluid and the porous domains as a continuum where momentum transport is governed by a single average equation, valid both in the homogeneous fluid and porous domains but also in the nonhomogeneous interfacial region where effective properties (permeability, porosity,...) are spatially dependent (Fig. 1). This single-domain model was recently theoretically derived, using the volume averaging method [13], for momentum [14] and convective mass transport [14]. It is worth mentioning that the derivation of the single average equation (or generalized transfer equation) can be free of length-scale constraint. Associated closure problems were also established and numerically solved for schematic interfacial structures in order to define the position-dependent effective transport properties. The single-domain has been widely used in numerical studies for practical configurations, but due to the difficulty to describe the local interfacial layer, the porous domain is generally assumed to be homogeneous and the transition between the fluid and the porous regions is represented by Heaviside functions; see Ref. [15] for the corresponding mathematical model.

In the two-domain approach, averaged transport equations in the fluid layer and the porous region, assumed to be homogeneous, are coupled at a *virtual interface*, also called "discrete interface" (or "dividing surface") through jump boundary conditions (Fig. 2). The derivations of these latter, the determination of associated jump coefficients and the location of the interface, are actually very challenging. Using Stokes and Darcy equations in the fluid and porous regions, respectively, Ref. [1] introduced a semiempirical slip velocity boundary condition, where the dimensionless slip coefficient is found to be dependent on the local structure of the interfacial region and the location of the interface [16]. The introduction of the slip jump condition was actually a mathematical necessity, but its relevance was proved due to the good agreement with the experiments (remember that the comparison was concerning the flow rate). The theoretical studies performed during the past two decades have shown that these jump boundary conditions actually represent the integration of transport phenomena over transition layer. The use of the

*benoit.goyeau@centralesupelec.fr

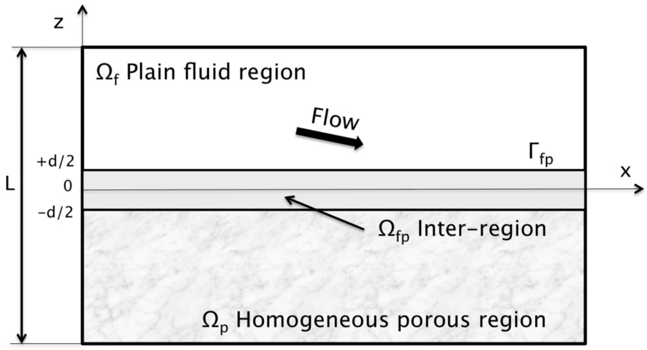

FIG. 1. One-domain modeling: nonhomogeneous continuous interregion of thickness d.

Darcy-Brinkman equation in the porous domain instead of Darcy's one gave rise to significant modeling alternatives. Indeed, assuming continuity of velocities at the interface, Refs. [17,18] derived, using the volume averaging method, a tangential stress jump condition whose jump coefficient is also found to be dependent on the local geometry of the interfacial region. Recently, Ref. [19] introduced a new methodology for the derivation of boundary conditions for both the velocity and the stress. The jump coefficients and the location of the discrete interface are obtained from the solution of an ancillary closure problem related to macroscopic deviations. A similar model involving two jump coefficients was previously obtained using matched asymptotic expansions method [20]. It is worth noting that both of the above methodologies are based on the combination of the single- and the two-domain approaches. In fact, jump boundary conditions in the two-domain approach actually result from the integration of transport phenomena in the interfacial transition layer of the single-domain approach [21]. This is also the case for the asymptotic analysis developed in the present study.

As previously said, most of the previous studies consider the 1D tangential flow and heat and mass transfer and very few attempts have been performed for bidimensional configurations where normal component of the velocity exists at the fluid-porous interface [22–24]. This is also the case for thin film flows on a porous substrate where height modulations give rise to nontangential velocities at the fluid-porous interface [25,26].

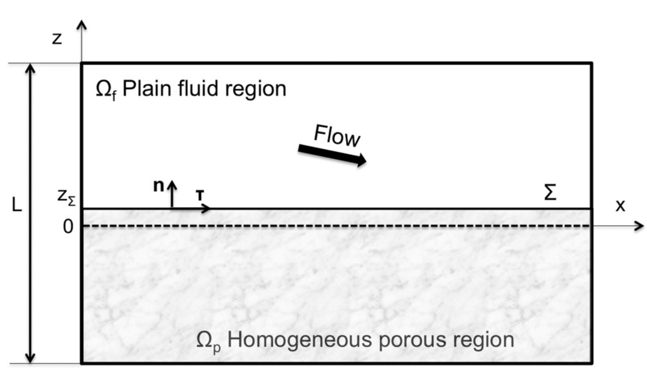

FIG. 2. Two-domain modeling: fictive dividing surface Σ whose location is at z_Σ.

The objective of the present study is to propose an *asymptotic modeling of a bidimensional* steady, noninertial, and incompressible viscous flow with normal transfer of momentum, energy, and mass in a fluid-porous single-domain Ω, see Fig. 1, in order to derive the jump conditions associated to the two-domain description. This analysis is based on the hypothesis $d/L \ll 1$, where d is the thickness of the transition layer Ω_{fp} while L represents a characteristic length scale of the system. As previously said, this modeling leads to replace the transport phenomena description in the thin inter-region by algebraic jump conditions at a fictive rectilinear interface Σ at the order one of d/L; see Fig. 2. Such an asymptotic modeling has been successfully carried out for other physical problems, e.g., scalar diffusion-reaction [27,28] or flow in fractured porous media [29,30]. Indeed, the asymptotic modeling for an elliptic problem neglecting the tangential derivative terms amounts to reduce a model with a diffuse or spread interface [31] to a model with a sharp interface [32]. By an *ad hoc* generalization to multidimensional vector problems, this has led to a *fictitious domain model* with the so-called *jump embedded boundary conditions*(JEBC) linking the jumps of both the stress tensor and the velocity or the displacement vector at the interface, proposed in Refs. [33–35] for viscous flow or elasticity problems.

This paper is organized as follows: Sec. II presents the governing equations for momentum transport in the fluid-porous system. In Sec. III, the multidimensional asymptotic model is developed and the jump boundary conditions at the fluid-porous interface are obtained. Comparisons with different existing models are detailed in Sec. IV.

II. FLUID-POROUS VISCOUS FLOW MODEL

Let us consider a two-dimensional [36] bounded domain $\Omega \subset \mathbb{R}^2$ composed of a pure homogeneous fluid region Ω_f and a saturated porous medium $\Omega_{fp} \cup \Omega_p$ separated by a physical interface Γ_{fp} (Fig. 1). The homogeneous part of the porous region Ω_p is characterized by its constant porosity ϕ^p and permeability tensor $\boldsymbol{K}^p$, while $\phi := \phi(x,z)$ and $\boldsymbol{K} := \boldsymbol{K}(\phi,\nabla\phi)$ are, respectively, the spatially dependent porosity and permeability tensor of the nonhomogeneous interfacial transition layer Ω_{fp}. For the sake of simplicity, Ω_{fp} is assumed to be quasirectilinear of constant thickness d (flat interface), and therefore the contribution of the curvature terms will be neglected in the present analysis. Nevertheless, d can be a slowly varying function of the longitudinal axis coordinate x (nonflat interface) and the present asymptotic model remains valid by taking $d = d(x)$. This is the case in many practical configurations, which will be developed in a separate study. Let us recall that the upscaling process from the pore scale ℓ_p to the macroscopic scale at the fluid porous interface is based on the scale separation $\ell_p \ll d$ (generally, $d \approx 20\ell_p$), since d is found to be twice the size of the averaging volume [14]. In addition, it is known that the pore length scale $\ell_p \approx \sqrt{K^p}$ and, therefore, d scales as $d = O(\sqrt{K^p})$, meaning that d is proportional to $\sqrt{K^p}$, i.e., $d \approx C\sqrt{K^p}$, where C is a dimensionless constant and $K^p := \|\boldsymbol{K}^p\|$. However, it is important to recall that in some porous structures, d/ℓ_p can be found of the order one [21], but we have in all practical configurations $d/L \ll 1$. Finally, it is worth recalling that the asymptotic analysis is based on the integration of the momentum transport over $\Omega_{\rm fp}$ giving rise to jump conditions at a fictive interface Σ whose location is not known *a priori*.

A. Homogeneous fluid and porous regions

The noninertial incompressible steady flow of a Newtonian fluid with constant mass density ρ and dynamic viscosity μ, is governed by the Stokes equations [37] in the fluid domain Ω_f:

$$\nabla \cdot \boldsymbol{v} = 0 \quad \text{in } \Omega_f, \tag{1}$$

$$-\mu\, \Delta \boldsymbol{v} + \nabla p = \rho\, \boldsymbol{f} \quad \text{in } \Omega_f. \tag{2}$$

Here, $\boldsymbol{f}$ denotes a body force like the gravitational one. The porous region $\Omega_{\rm fp} \cup \Omega_p$ is much more complex and macroscopic momentum modeling deserves to be explained. Let us first consider the homogeneous porous structure Ω_p often characterized by three length scales: the size of the solid elements ℓ, the size of the representative unit cell η, and the macroscopic scale L [38]. On this basis, the derivation of the average momentum equations from the Stokes equations has been the subject of many studies using different geometries and methodologies such as asymptotic expansions and multiscale homogenization, either deterministic [39–48] or stochastic homogenization for random media [49,50], or also volume averaging [13,51–53]. Let us emphasize that, whatever the methodology used and before any simplification related to scale separations and limit behaviors, the stationary noninertial macroscopic momentum equation for viscous flow in homogeneous porous media is governed by the Darcy-Brinkman form [54,55]:

$$\nabla \cdot \boldsymbol{v} = 0 \quad \text{in } \Omega_p, \tag{3}$$

$$-\widetilde{\mu}\, \Delta \boldsymbol{v} + \mu\, \boldsymbol{K}_d^{-1} \cdot \boldsymbol{v} + \nabla p = \rho\, \boldsymbol{f}, \quad \text{in } \Omega_p, \tag{4}$$

where $\widetilde{\mu}$ is the effective viscosity of Brinkman's term, whereas $\boldsymbol{K}_d$ is the permeability tensor of Darcy's term; see, e.g., Ref. [56] for the use of such a Brinkman model. Remember that in Eq. (4), $\boldsymbol{v}$ represents the superficial average velocity (also classically called the filtration velocity), while the pressure p refers to the intrinsic average pressure. It is important to note that all the asymptotic analyses that have been performed show that the viscous diffusion term (Brinkman's term) is *negligible* compared to the friction term (Darcy's term) in most porous media, except for porous structures with high porosity and permeability values. This is the reason why, except for this latter case, Eq. (4) reduces to Darcy's law [57]:

$$\mu\, \boldsymbol{K}_d^{-1} \cdot \boldsymbol{v} + \nabla p = \rho\, \boldsymbol{f} \quad \text{in } \Omega_p. \tag{5}$$

More precisely, it is proved in Brillard [44], Rubinstein [49,50], Marchenko and Khruslov [58], that the macroscopic equation converges to Brinkman's law, Eq. (4), as far as $\ell/\eta \to 0$ when $\eta \to 0$; with $\ell = O(\eta)$, Darcy's law, Eq. (5), is obtained at convergence when $\eta \to 0$. Moreover, there exists a critical size of the solid inclusions: $\ell^c := C\,\eta^3$ in 3D or $\ell^c := \exp(-C\,\eta^{-2})$ in 2D with some $C > 0$ [41,44,46,47]. When $\ell/\ell^c \to a > 0$, Brinkman's law is obtained at convergence for $\eta \to 0$; when $a = +\infty$, it leads to Darcy's law, and the Stokes equation is recovered when $a = 0$. For very high porosity and permeability values, due to the size of the solid elements when $\ell \ll O(\eta^3)$ [41], the friction forces strongly decrease, and for the limiting case where $\boldsymbol{K}_d \to \infty$ ($\phi \to 1$), Eq. (4) asymptotically tends toward the Stokes equation. It is worth mentioning that, in this case, the effective viscosity also tends to the fluid viscosity [21]. Besides, the large majority of studies devoted to the determination of the effective viscosity have concerned sparse porous structures [59–66], where all expressions are found to be close to the linear Einstein's law [67]: $\widetilde{\mu} = \mu[1 + 2.5(1-\phi)]$ that has been established for dilute suspensions. Attempts have been made for denser beds of spheres with or without inertia [16,59,65,66], but contradictory behaviors were obtained. This is, in fact, without any consequence since the Brinkman term only influences the flow at high porosity and permeability values. In conclusion, this brief review shows that the Darcy-Brinkman Eq. (4) is actually valid whatever the type of porous microstructure, but the Brinkman term is generally negligible and Darcy's law is sufficient except for very sparse porous structures.

B. Heterogeneous porous region

The porous medium under consideration in the present analysis contains a thin heterogeneous interfacial porous layer $\Omega_{\rm fp}$, where averaged properties are continuously spatially dependent (evolving heterogeneities). Indeed, the porosity varies from ϕ^p in the homogeneous porous region Ω_p to 1 in the fluid Ω_f, while the permeability varies from $\boldsymbol{K}^p$ to ∞. Therefore, in the large part of the interfacial porous layer, the Brinkman term is negligible but becomes important in the vicinity of the plain fluid region. In this transition layer, the Brinkman term allows the continuous evolution of the momentum transport between the homogeneous fluid and porous regions. Moreover, it has been shown that for nonhomogeneous porous media, the volume averaging method leads to an additional Brinkman term involving porosity gradients [[13], Chap. 4]:

$$-\widetilde{\mu}\, \Delta \boldsymbol{v} + \mu\, \phi^{-1} \nabla \phi \cdot \nabla(\phi^{-1} \boldsymbol{v}) + \mu\, \boldsymbol{K}_d^{-1}(\phi) \cdot \boldsymbol{v} + \nabla p = \rho\, \boldsymbol{f} \quad \text{in } \Omega_{\rm fp}. \tag{6}$$

In Eq. (6), the permeability tensor $\boldsymbol{K}_d(\phi)$ *a priori* depends on the porosity and *its variations*. However, it is worth mentioning that whatever the dependance of $\boldsymbol{K}_d(\phi)$, the analysis performed in the present study remains relevant since the objective is to derive a general form of jump interface conditions for multi-dimensional flows without providing an explicit form of the associated coefficients. This is the reason why, despite the evolving heterogeneities in the transition layer, the scale separation is assumed to be satisfied, i.e., $\ell_p \ll L_\phi, L_{\boldsymbol{v}}$ (ℓ_p and $L_\phi, L_{\boldsymbol{v}}$ being the local and macroscopic length scales, respectively). Therefore, the influence of the porosity gradients can be neglected for the determination of the permeability tensor $\boldsymbol{K}_d(\phi)$. For convenience, Eq. (6) can be written under the conservative form:

$$-\nabla \cdot (\widetilde{\mu} \nabla \boldsymbol{v}) + \mu \boldsymbol{K}^{-1} \cdot \boldsymbol{v} + \nabla p = \rho\, \boldsymbol{f} \quad \text{in } \Omega_{\rm fp}, \tag{7}$$

where the effective viscosity $\widetilde{\mu}$ is equal to $\widetilde{\mu} := \mu/\phi$ [13] and the equivalent permeability tensor $\boldsymbol{K} := \boldsymbol{K}(\phi, \nabla\phi)$ is defined by [68]

$$K(\phi,\nabla\phi)^{-1} := K_d(\phi)^{-1} - \phi^{-3}\|\nabla\phi\|^2 I, \quad (8)$$

where I is the unit tensor, since we have

$$-\frac{\mu}{\phi}\Delta v + \frac{\mu}{\phi}\nabla\phi\cdot\nabla\left(\frac{1}{\phi}v\right) = -\frac{\mu}{\phi}\Delta v + \frac{\mu}{\phi^2}\nabla\phi\cdot\nabla v - \frac{\mu}{\phi^3}\|\nabla\phi\|^2 v = -\nabla\cdot\left(\frac{\mu}{\phi}\nabla v\right) - \frac{\mu}{\phi^3}\|\nabla\phi\|^2 v.$$

It is shown in Appendix A that Eq. (8) actually defines $K(\phi,\nabla\phi)$ as a symmetric and positive definite tensor written as

$$K(\phi,\nabla\phi) = \begin{pmatrix} K_\tau & K_{\tau n} \\ K_{n\tau} & K_n \end{pmatrix}.$$

Since there is no porosity gradient in Ω_p, this equation can be used in $\Omega_{\mathrm{fp}} \cup \Omega_p$. Under these circumstances, the steady form of the noninertial incompressible viscous flow inside the fluid-porous system in Ω is defined by

$$\begin{aligned} \nabla\cdot v &= 0, && \text{in } \Omega,\\ -\nabla\cdot\sigma(v,p) &= \rho f, && \text{in } \Omega_f,\\ -\nabla\cdot\sigma(v,p) + \mu K^{-1}\cdot v &= \rho f, && \text{in } \Omega_{\mathrm{fp}}\cup\Omega_p, \end{aligned} \quad (9)$$

where $\sigma(v,p)$ represents the pseudostress tensor for a newtonian fluid defined by

$$\sigma(v,p) := -p\, I + \widetilde{\mu}\,\nabla v = -p\, I + \frac{\mu}{\phi}\nabla v.$$

Furthermore, the continuity of both the stress and velocity vectors apply at the interface Γ_{fp}, that is no jump, n being the unit normal vector oriented from porous to fluid regions:

$$[\![v]\!]_{\Gamma_{\mathrm{fp}}} = 0 \quad \text{and} \quad [\![\sigma(v,p)\cdot n]\!]_{\Gamma_{\mathrm{fp}}} = 0 \quad \text{on } \Gamma_{\mathrm{fp}}. \quad (10)$$

This set of equations must be supplemented by adequate boundary conditions on the external frontier $\Gamma := \partial\Omega$ supposed to be partitioned in two parts as $\Gamma = \Gamma_D \cup \Gamma_N$. For example, we usually impose the following Dirichlet condition for the velocity on Γ_D and an open condition given in stress on the Neumann boundary Γ_N, ν being the external unit normal vector on Γ_N:

$$\begin{aligned} v &= v_D, && \text{on } \Gamma_D,\\ \sigma(v,p)\cdot \nu_{|\Gamma_N} &= g, && \text{on } \Gamma_N. \end{aligned} \quad (11)$$

The fluid-porous flow model Eqs. (9)–(11) can be reformulated using a *single-domain formulation* where a single generalized Brinkman equation with variable coefficients is used to describe the fluid-porous flow inside the whole domain Ω. For instance, a continuous smooth variation of the permeability is proposed in Ref. [12] with a tanh function from the nominal permeability in the porous medium to infinity in the plain fluid; see also Ref. [69]. We also refer to Ref. [70], where discontinuous permeability variations are introduced with $K^s := \varepsilon\, I$ in an impermeable solid region (and possibly a viscosity coefficient $\mu^s := 1/\varepsilon$), a permeability tensor K^p in the porous region and $K^f := 1/\varepsilon\, I$ in the pure fluid domain Ω_f, $0 < \varepsilon \ll 1$ being a small penalty parameter that tends to zero. In that case, the continuity of both the stress and velocity vectors was implicitly assumed on the physical interface separating the pure fluid region from the porous medium. Hence, we can consider the following fictitious domain model to govern the viscous flow inside the present fluid-porous system in Ω:

$$\begin{aligned} \nabla\cdot v_\varepsilon &= 0, && \text{in } \Omega,\\ -\nabla\cdot\sigma(v_\varepsilon,p_\varepsilon) + \mu\, K_\varepsilon^{-1}\cdot v_\varepsilon &= \rho f, && \text{in } \Omega,\\ \text{with: } K_\varepsilon &:= K^p, && \text{in } \Omega_p,\\ K_\varepsilon &:= K(\phi,\nabla\phi), && \text{in } \Omega_{\mathrm{fp}},\\ K_\varepsilon &:= \frac{1}{\varepsilon} I, && \text{in } \Omega_f,\\ \widetilde{\mu} := \frac{\mu}{\phi} \ \text{in } \Omega, \quad \text{and} \quad \phi^f &:= 1 && \text{in } \Omega_f. \end{aligned} \quad (12)$$

Let us point out that the stress and velocity continuity conditions on Γ_{fp} in Eq. (10) are now inherently and implicitly included within the formulation of Eq. (12). This is proved within a suitable weak formulation by Angot [15]. Then, it is no more necessary to write them explicitly. We thus refer to Angot [15] for the mathematical analysis of the models Eqs. (9), (10), and (12). In particular, it is proved that the solution $(v_\varepsilon, p_\varepsilon)$ of the fictitious domain model Eq. (12) tends to the solution (v,p) of the primary fluid-porous model Eqs. (9) and (10) when the penalty parameter ε tends to zero. More precisely, we have the following error estimate:

$$\|v_\varepsilon - v\|_{H^1(\Omega)} + \|p_\varepsilon - p\|_{L^2(\Omega)} \leqslant C\,\varepsilon,$$

where C only depends on the data and not on ε, $L^2(\Omega)$ denotes the Lebesgue space of square-integrable functions, and $H^1(\Omega)$ is the standard Sobolev space. We also refer to Ref. [71] for the corresponding numerical method with finite volumes to efficiently solve such fictitious domain models.

III. THEORETICAL DERIVATION OF THE ASYMPTOTIC MODEL

As underlined in the abstract, the main objective of the present work is twofold.

(1) First, to propose a general and unified framework to theoretically derive the multidimensional form of the jump interface conditions (at the macroscopic scale L), depending on whether the flow in the porous medium Ω_p is described either by Brinkman's law or Darcy's law and we study both cases (see Sec. II A); the results being, respectively, in Sec. III D 1 or III D 2.

The analysis is based on an asymptotic modeling of a very thin interfacial and nonhomogeneous porous layer Ω_{fp}, the thickness of which $d = O(\sqrt{K^p})$ being such that $d/L \ll 1$ (see introduction of Sec. II). This enables us to propose an approximate but multidimensional interface model up to the order $O(d/L)$, which is original in our knowledge.

(2) Second, to recover all the tangential interface conditions existing in the literature when there is no transverse flow with $v\cdot n_{|\Sigma} = 0$, each having its own domain of validity, as detailed in Sec. IV.

The Brinkman equation in Eq. (9) is further averaged over the thickness d of the interfacial layer $\Omega_{\rm fp}$ in Sec. III B; see Fig. 1. The coupled heat (or mass) transfer problem inside $\Omega_{\rm fp}$ is considered in Sec. III C.

A. Definitions and approximations

Let $\boldsymbol{n}$ be a unit normal vector on the interface Σ arbitrarily oriented from Ω_p to Ω_f and $\boldsymbol{\tau}$ be a unit tangential vector on Σ; see Fig. 2. For any quantity ψ defined all over Ω, the restrictions on Ω_f or Ω_p are, respectively, denoted by $\psi^f := \psi_{|\Omega_f}$ and $\psi^p := \psi_{|\Omega_p}$ [72]. For a function ψ having a jump on Σ, let ψ^- and ψ^+ be the traces of ψ^p and ψ^f on each side of Σ, respectively, and the jump of ψ on Σ oriented by $\boldsymbol{n}$ and the arithmetic mean of traces of ψ are defined by

$$[\![\psi]\!]_\Sigma := \psi^+ - \psi^- = (\psi^f - \psi^p)_{|\Sigma},$$
$$\text{and} \quad \overline{\psi}_\Sigma := \tfrac{1}{2}(\psi^+ + \psi^-) = \tfrac{1}{2}(\psi^f + \psi^p)_{|\Sigma}. \quad (13)$$

Thus, we have also

$$\psi^f_{|\Sigma} := \psi^+ = \overline{\psi}_\Sigma + \tfrac{1}{2}[\![\psi]\!]_\Sigma,$$
$$\text{and} \quad \psi^p_{|\Sigma} := \psi^- = \overline{\psi}_\Sigma - \tfrac{1}{2}[\![\psi]\!]_\Sigma. \quad (14)$$

However, the great motivation to introduce the quantities $[\![\psi]\!]_\Sigma$ and $\overline{\psi}_\Sigma$ for expressing the jump interface conditions only with these terms was early given by Angot [27]. Indeed, when there is no jump of the function ψ across Σ, we have $[\![\psi]\!]_\Sigma = 0$ and then $\overline{\psi}_\Sigma = \psi_{|\Sigma}$, and hence the corresponding interface conditions should easily degenerate to satisfy the continuity of ψ across Σ. Furthermore, this also greatly simplifies both the mathematical and numerical analysis, since the model has a symmetric form; see also Refs. [28,33].

For a noncentered interface Σ as in Fig. 2, we shall use the weighted mean:

$$\begin{aligned}\overline{\psi}^w_\Sigma &:= \frac{d/2 - z_\Sigma}{d}\,\psi^- + \frac{d/2 + z_\Sigma}{d}\,\psi^+\\ &= \left(\frac{1}{2} - \xi\right)\psi^- + \left(\frac{1}{2} + \xi\right)\psi^+\\ &= \overline{\psi}_\Sigma + \xi\,[\![\psi]\!]_\Sigma,\\ \text{with} \quad -\frac{1}{2} &\leqslant \xi := \frac{z_\Sigma}{d} \leqslant \frac{1}{2}. \end{aligned} \quad (15)$$

Besides, for any quantity k, the arithmetic and harmonic means over the thickness of $\Omega_{\rm fp}$, respectively, are given by

$$\langle k\rangle(x) := \frac{1}{d(x)}\int_{-d/2}^{d/2} k(x,z)\,dz,$$
$$\langle k\rangle^h(x) := \left(\frac{1}{d(x)}\int_{-d/2}^{d/2}\frac{dz}{k(x,z)}\right)^{-1} = \frac{1}{\langle\frac{1}{k}\rangle}, \quad (16)$$

the latter being more accurate when k denotes a diffusion or permeability coefficient; see Lemma 1 and Remark 1 in Appendix B.

By reducing the thin interfacial region $\Omega_{\rm fp}$ to a fictive interface Σ located in the middle ($z_\Sigma = 0$), each physical variable ψ_Σ on Σ will be then defined by its cross average value $\langle\psi\rangle$ over the thickness of $\Omega_{\rm fp}$. As a consequence, the modeling error made in the asymptotic interface model is of the order of $O(d/L)$, i.e., of first-order. If we now choose to approach the corresponding integral by the trapezoidal quadrature rule, which is an approximation at the order of $O(d^3)$ for a smooth function, see Lemma 3 in Appendix B, we have

$$\begin{aligned}\psi_\Sigma(x) &:= \frac{1}{d}\int_{-d/2}^{d/2}\psi(x,z)\,dz\\ &= \frac{1}{2}(\psi(x,-d/2) + \psi(x,d/2)) + O(d^2)\\ &= \overline{\psi}_\Sigma + O(d^2) \approx \overline{\psi}_\Sigma.\end{aligned}$$

For the jump quantities, we have also at the first-order in $O(d/L)$:

$$\psi(x,d/2) - \psi(x,-d/2) = [\![\psi]\!]_\Sigma + O(d/L) \approx [\![\psi]\!]_\Sigma.$$

As mentioned in the Introduction, the jump boundary conditions at the interface between a fluid and a porous region depend on the location of the fictive interface Σ [19,20]. A reasonable estimation for this location can be the middle of the interfacial layer $\Omega_{\rm fp}$, but a more general choice would be to consider a noncentered position. In that case, ψ_Σ remains defined by $\psi_\Sigma := \langle\psi\rangle$, but a noncentered "midpoint" quadrature rule is used to approximate the integral which is only at the order of $O(d^2)$; see Lemma 2.

Thus, we have

$$\begin{aligned}\psi_\Sigma(x) &:= \frac{1}{d}\int_{-d/2}^{d/2}\psi(x,z)\,dz\\ &= \psi(x,z_\Sigma) + O(d) = \overline{\psi}^w_\Sigma + O(d)\\ &\approx \overline{\psi}^w_\Sigma = \overline{\psi}_\Sigma + \xi\,[\![\psi]\!]_\Sigma.\end{aligned}$$

Hereafter, all the vector or tensor quantities are written within the local curvilinear reference basis $(\boldsymbol{\tau},\boldsymbol{n})$. For example, a vector quantity $\boldsymbol{v}$ reads

$$\boldsymbol{v} = v_\tau\,\boldsymbol{\tau} + v_n\,\boldsymbol{n} \quad \text{with} \quad v_\tau := \boldsymbol{v}\cdot\boldsymbol{\tau}, \quad v_n := \boldsymbol{v}\cdot\boldsymbol{n}.$$

Since the interface Σ is supposed to be quasirectilinear, the contribution of the curvature terms will be neglected everywhere and the curvilinear coordinates are thus (x,z). Then, $\boldsymbol{\nabla}_{\boldsymbol{\tau}}$ denotes the tangential nabla operator, whereas ∂_n or ∂_z denotes the normal partial derivative. We use the dimensional analysis to compare the orders of magnitude and justify the approximations by choosing the reference velocity V being, for example, the value of the uniform incoming flow at infinity. This will enable us to neglect the contribution of all tangential derivatives at the interface up to the order $O(d/L)$.

B. Jump interface conditions for the stress and velocity vectors

The asymptotic model for the momentum transfer is derived by integrating Eqs. (9), (10), or (12) over the thickness of the interfacial layer $\Omega_{\rm fp}$ using the hypothesis $d/L \ll 1$ and the approximations detailed in Sec. III A. Then, the averaged transfer is described at the fictive dividing interface Σ through suitable algebraic jump interface conditions at the first-order in $O(d/L)$. We first consider the simplest choice when the fictive interface Σ is centered inside $\Omega_{\rm fp}$, i.e., with the dimensionless coordinate $\xi := z_\Sigma/d = 0$. The modifications involved by $\xi \neq 0$ with $-1/2 \leqslant \xi \leqslant 1/2$ are later given in Sec. III D 3.

1. Jump condition for mass conservation

By integrating the continuity equation in Eqs. (9) or (12) over the thickness of the interfacial region Ω_{fp}, we have

$$\int_{-d/2}^{d/2} \nabla\cdot\boldsymbol{v}\,dz = 0.$$

Since the left-hand side reads

$$\begin{aligned}\int_{-d/2}^{d/2} \nabla\cdot\boldsymbol{v}\,dz &= \int_{-d/2}^{d/2} \nabla_\tau\cdot\boldsymbol{v}\,dz + \int_{-d/2}^{d/2} \nabla_n\cdot\boldsymbol{v}\,dz\\ &= \int_{-d/2}^{d/2} \nabla_\tau\cdot\boldsymbol{v}\,dz + \int_{-d/2}^{d/2} \partial_n(\boldsymbol{v}\cdot\boldsymbol{n})\,dz\\ &= \nabla_\tau\cdot(d\,\langle\boldsymbol{v}\cdot\boldsymbol{\tau}\rangle)\\ &\quad+(\boldsymbol{v}\cdot\boldsymbol{n}(x,d/2)-\boldsymbol{v}\cdot\boldsymbol{n}(x,-d/2)),\end{aligned}$$

the equation becomes

$$\nabla_\tau\cdot(d\,\langle\boldsymbol{v}\cdot\boldsymbol{\tau}\rangle)+(\boldsymbol{v}\cdot\boldsymbol{n}(x,d/2)-\boldsymbol{v}\cdot\boldsymbol{n}(x,-d/2))=0.$$

Using the trapezoidal quadrature rule to approximate the integral in the first term, we get the equality

$$\underbrace{\nabla_\tau\cdot(d\,\overline{\boldsymbol{v}\cdot\boldsymbol{\tau}}_\Sigma)}_{O(V\,d/L)}+\underbrace{[\![\boldsymbol{v}\cdot\boldsymbol{n}]\!]_\Sigma}_{O(V)}=0.$$

By neglecting now the first term, which is a tangential derivative of the order of $O(V\,d/L)$, with respect to the other term in $O(V)$, it yields the algebraic jump interface condition below at the first-order in $O(V\,d/L)$:

$$[\![\boldsymbol{v}\cdot\boldsymbol{n}]\!]_\Sigma = 0 \quad \text{on} \quad \Sigma. \tag{17}$$

As naturally expected [22,23], the incompressible flow produces no jump of normal velocity component when there is no mass source, and we have $[\![\boldsymbol{v}\cdot\boldsymbol{n}]\!]_\Sigma = 0$ and then $\overline{\boldsymbol{v}\cdot\boldsymbol{n}}_\Sigma = \boldsymbol{v}\cdot\boldsymbol{n}_{|\Sigma}$. This is recently confirmed both by homogenization and direct numerical simulation in Ref. [73].

2. Jump conditions for momentum transport

The integration of the momentum equation in Eq. (9) or Eq. (12) over the thickness of the interfacial region Ω_{fp} gives

$$\begin{aligned}-\int_{-d/2}^{d/2} \nabla\cdot\boldsymbol{\sigma}(\boldsymbol{v},p)\,dz + \int_{-d/2}^{d/2}\mu\,\boldsymbol{K}(\phi,\nabla\phi)^{-1}\cdot\boldsymbol{v}\,dz\\ = \int_{-d/2}^{d/2}\rho\,\boldsymbol{f}\,dz = d\,\langle\rho\,\boldsymbol{f}\rangle.\end{aligned}\tag{18}$$

For the first term in Eq. (18), we have in the 2D tensor form

$$\boldsymbol{\sigma}(\boldsymbol{v},p) := \begin{pmatrix}\sigma_\tau & \sigma_{\tau n}\\ \sigma_{n\tau} & \sigma_n\end{pmatrix},$$

hence

$$\nabla\cdot\boldsymbol{\sigma}(\boldsymbol{v},p) := \left(\sum_{i,j=1}^{2}\partial_{x_j}\sigma_{ij}\right) = \begin{pmatrix}\partial_\tau\sigma_\tau+\partial_n\sigma_{\tau n}\\ \partial_\tau\sigma_{n\tau}+\partial_n\sigma_n\end{pmatrix}.$$

Thus, neglecting the tangential derivatives in $O(d/L)$, it yields up to $O(d/L)$

$$\begin{aligned}-\int_{-d/2}^{d/2}\nabla\cdot\boldsymbol{\sigma}(\boldsymbol{v},p)\,dz &= -\begin{pmatrix}\partial_\tau(d\,\langle\sigma_\tau\rangle)+[\![\sigma_{\tau n}]\!]_\Sigma\\ \partial_\tau(d\,\langle\sigma_{n\tau}\rangle)+[\![\sigma_n]\!]_\Sigma\end{pmatrix}\\ &\approx -\begin{pmatrix}[\![\sigma_{\tau n}]\!]_\Sigma\\ [\![\sigma_n]\!]_\Sigma\end{pmatrix} = -[\![\boldsymbol{\sigma}(\boldsymbol{v},p)\cdot\boldsymbol{n}]\!]_\Sigma.\end{aligned}$$

Indeed, we have to compare the tangential derivatives:

$$|\partial_\tau(d\,\langle\sigma_\tau\rangle)| = O\left(\frac{\mu\,V}{L}\,\frac{d}{L}\right),$$

$$|\partial_\tau(d\,\langle\sigma_{n\tau}\rangle)| = O\left(\frac{\mu\,V}{L}\,\frac{d}{L}\right),$$

to the term

$$|[\![\boldsymbol{\sigma}(\boldsymbol{v},p)\cdot\boldsymbol{n}]\!]_\Sigma| = O\left(\frac{\mu\,V}{L}\right).$$

The last term of Darcy's drag in the left-hand side of Eq. (18) is estimated in vector form using the approximation of the generalized average from Corollary 1 and proved in Lemma 4 in Appendix B. It yields

$$\begin{aligned}\int_{-d/2}^{d/2}\mu\,\boldsymbol{K}^{-1}\cdot\boldsymbol{v}\,dz &= \mu\,d\langle\boldsymbol{K}^{-1}\rangle\cdot\overline{\boldsymbol{v}}_\Sigma\\ &\quad+O(\mu\,\|\boldsymbol{K}^{-1}\|\,\|\nabla\boldsymbol{v}\|\,d^2).\end{aligned}$$

Thus, it amounts to neglect the error term of order $O(\mu\,V\,d/K\,d/L)$ compared to the term in $O(\mu\,V\,d/K)$, which holds. It gives then the approximation

$$\int_{-d/2}^{d/2}\mu\,\boldsymbol{K}^{-1}\cdot\boldsymbol{v}\,dz \approx \mu\,d\langle\boldsymbol{K}^{-1}\rangle\cdot\overline{\boldsymbol{v}}_\Sigma.$$

Hence, we get the following approximation of Eq. (18) in vector form up to $O(d/L)$:

$$[\![\boldsymbol{\sigma}(\boldsymbol{v},p)\cdot\boldsymbol{n}]\!]_\Sigma = \mu\,d\,\boldsymbol{K}_\Sigma^{-1}\cdot\overline{\boldsymbol{v}}_\Sigma - d\,\langle\rho\,\boldsymbol{f}\rangle \quad \text{on} \quad \Sigma,$$

$\boldsymbol{K}_\Sigma$ being the effective permeability defined by

$$\boldsymbol{K}_\Sigma := \langle\boldsymbol{K}(\phi,\nabla\phi)^{-1}\rangle^{-1} := \langle\boldsymbol{K}(\phi,\nabla\phi)\rangle^h, \quad \text{on}\ \Sigma. \tag{19}$$

For instance, in the case of a diagonal permeability tensor $\boldsymbol{K}(\phi,\nabla\phi)$ inside Ω_{fp}, the effective permeability tensor on Σ reads

$$\boldsymbol{K}_\Sigma := \begin{pmatrix}\langle K_\tau(\phi,\nabla\phi)\rangle^h & 0\\ 0 & \langle K_n(\phi,\nabla\phi)\rangle^h\end{pmatrix}.$$

Equation (19) physically means the force balance on Σ. Moreover, Eq. (19) can be viewed as a generalized form of the stress jump interface condition derived by Ochoa-Tapia and Whitaker [17], for multidimensional flows with $[\![\boldsymbol{v}\cdot\boldsymbol{n}]\!]_\Sigma = 0$ from Eq. (17) and $[\![\boldsymbol{v}\cdot\boldsymbol{\tau}]\!]_\Sigma \neq 0$; see Sec. IV B.

Since the above interface condition expresses the jump of the pseudostress vector on Σ, we also integrate over Ω_{fp} the equation defining $\boldsymbol{\sigma}(\boldsymbol{v},p)\cdot\boldsymbol{n}$:

$$\boldsymbol{\sigma}(\boldsymbol{v},p)\cdot\boldsymbol{n} := -p\,\boldsymbol{n}+\widetilde{\mu}\,\nabla\boldsymbol{v}\cdot\boldsymbol{n}\ \text{in}\ \ \Omega_{\text{fp}},\ \text{with}\ \ \widetilde{\mu} := \frac{\mu}{\phi}, \tag{20}$$

in order to obtain a suitable approximation of the mean stress vector on Σ.

By approaching the two sides of the equality Eq. (20) with the trapezoidal rule from Lemma 3, it yields on one hand

$$\int_{-d/2}^{d/2} \boldsymbol{\sigma}(\boldsymbol{v},p)\cdot\boldsymbol{n}\,dz = d\,\langle\boldsymbol{\sigma}(\boldsymbol{v},p)\cdot\boldsymbol{n}\rangle \approx d\,\overline{\boldsymbol{\sigma}(\boldsymbol{v},p)\cdot\boldsymbol{n}}_\Sigma. \tag{21}$$

On the other hand, we have

$$\int_{-d/2}^{d/2} \boldsymbol{\sigma}(\boldsymbol{v},p)\cdot\boldsymbol{n}\,dz = -d\,\langle p\rangle\,\boldsymbol{n} + \int_{-d/2}^{d/2}\frac{\mu}{\phi}\,\nabla\boldsymbol{v}\cdot\boldsymbol{n}\,dz$$
$$\approx -d\,\overline{p}_\Sigma\,\boldsymbol{n} + \int_{-d/2}^{d/2}\frac{\mu}{\phi}\,\nabla\boldsymbol{v}\cdot\boldsymbol{n}\,dz. \tag{22}$$

It remains to approximate the last term with the tensor $\nabla\boldsymbol{v}$ reading in 2D

$$\nabla\boldsymbol{v} := \left(\partial_{x_j} v_i\right)_{1\leqslant i,j\leqslant 2} = \begin{pmatrix}\partial_\tau\boldsymbol{v}\cdot\boldsymbol{\tau} & \partial_n\boldsymbol{v}\cdot\boldsymbol{\tau}\\ \partial_\tau\boldsymbol{v}\cdot\boldsymbol{n} & \partial_n\boldsymbol{v}\cdot\boldsymbol{n}\end{pmatrix}.$$

Then, the last term in Eq. (22) is approximated as follows by Corollary 1 and neglecting again the tangential derivatives up to $O(d/L)$, as in Sec. III B 1:

$$\int_{-d/2}^{d/2}\frac{\mu}{\phi}\,\nabla\boldsymbol{v}\cdot\boldsymbol{n}\,dz \approx \mu\,\langle\phi^{-1}\rangle\int_{-d/2}^{d/2}\nabla\boldsymbol{v}\cdot\boldsymbol{n}\,dz$$
$$\approx \mu\,\langle\phi^{-1}\rangle\begin{pmatrix}[\![\boldsymbol{v}\cdot\boldsymbol{\tau}]\!]_\Sigma\\ [\![\boldsymbol{v}\cdot\boldsymbol{n}]\!]_\Sigma\end{pmatrix}.$$

Indeed, using Corollary 1, the terms including the tangential derivatives scale as

$$|\mu\,\partial_\tau(d\,\overline{\boldsymbol{v}\cdot\boldsymbol{\tau}}_\Sigma)| = O\left(\mu\,V\,\frac{d}{L}\right),$$
$$|\mu\,\partial_\tau(d\,\overline{\boldsymbol{v}\cdot\boldsymbol{n}}_\Sigma)| = O\left(\mu\,V\,\frac{d}{L}\right),$$

and can be thus neglected with respect to the jump terms

$$|\mu\,[\![\boldsymbol{v}\cdot\boldsymbol{\tau}]\!]_\Sigma| = O(\mu\,V),\quad |\mu\,[\![\boldsymbol{v}\cdot\boldsymbol{n}]\!]_\Sigma| = O(\mu\,V);$$

the error term from Corollary 1 being in $O(\mu\,\|\nabla\boldsymbol{v}\|\,d^2) = O(\mu\,V\,d^2/L)$. Moreover, the modeling error to get the jumps on Σ is also in $O(\mu\,V\,d/L)$, as explained in Sec. III A, and is thus negligible in front of the other terms in $O(\mu\,V)$.

Hence, combining Eqs. (21) and (22) with the previous approximations, we get the condition for the mean viscous stress vector on Σ up to $O(d/L)$:

$$\overline{\boldsymbol{\sigma}(\boldsymbol{v},p)\cdot\boldsymbol{n}}_\Sigma + \overline{p}_\Sigma\,\boldsymbol{n} = \frac{\mu}{\phi_\Sigma}\,\frac{[\![\boldsymbol{v}]\!]_\Sigma}{d}\quad\text{on}\quad\Sigma, \tag{23}$$

where ϕ_Σ is the effective surface porosity on Σ:

$$\phi_\Sigma := \frac{1}{\langle\phi^{-1}\rangle} := \langle\phi\rangle^h. \tag{24}$$

We can observe that the mean viscous stress vector $\overline{\boldsymbol{\sigma}_v(\boldsymbol{v})\cdot\boldsymbol{n}}_\Sigma := \overline{\boldsymbol{\sigma}(\boldsymbol{v},p)\cdot\boldsymbol{n}}_\Sigma + \overline{p}_\Sigma\,\boldsymbol{n}$ on Σ linearly depends on a constant normal gradient of the velocity vector across Σ. Moreover, using $[\![\boldsymbol{v}\cdot\boldsymbol{n}]\!]_\Sigma = 0$ from Eq. (17), Eq. (23) can be viewed as a generalized form of the velocity jump interface condition of Beavers and Joseph [1] for multidimensional flows; see Sec. IV A.

3. On the pressure jump on Σ

The existence of a pressure jump at a fluid-porous interface in the case of a transverse or oblique flow has been a subject of controversy for a long time; see, e.g., Refs. [22,24,74]. However, this jump was recently confirmed using both homogenization in Refs. [73,75] and direct numerical simulations [73,76].

The present asymptotic model allows us to calculate the pressure jump on Σ using Eqs. (20) and (19). On the one hand, we have with the latter

$$[\![\boldsymbol{\sigma}(\boldsymbol{v},p)\cdot\boldsymbol{n}]\!]_\Sigma\cdot\boldsymbol{n} = \mu\,d\big(\boldsymbol{K}_\Sigma^{-1}\cdot\overline{\boldsymbol{v}}_\Sigma\big)\cdot\boldsymbol{n} - d\,\langle\rho\,\boldsymbol{f}\cdot\boldsymbol{n}\rangle.$$

On the other hand, we have also from Eq. (20) and the calculations in Sec. III B 2

$$[\![\boldsymbol{\sigma}(\boldsymbol{v},p)\cdot\boldsymbol{n}]\!]_\Sigma\cdot\boldsymbol{n} = -[\![p]\!]_\Sigma + \left[\!\!\left[\frac{\mu}{\phi}\,\nabla\boldsymbol{v}\cdot\boldsymbol{n}\right]\!\!\right]_\Sigma\cdot\boldsymbol{n}$$
$$= -[\![p]\!]_\Sigma + \mu\left[\!\!\left[\frac{1}{\phi}\,\partial_n(\boldsymbol{v}\cdot\boldsymbol{n})\right]\!\!\right]_\Sigma.$$

Combining the above equations, we get the equation for the pressure jump on Σ up to $O(d/L)$:

$$\mu\big(\boldsymbol{K}_\Sigma^{-1}\cdot\overline{\boldsymbol{v}}_\Sigma\big)\cdot\boldsymbol{n} + \frac{[\![p]\!]_\Sigma}{d} - \mu\,\frac{[\![\frac{1}{\phi}\,\partial_n(\boldsymbol{v}\cdot\boldsymbol{n})]\!]_\Sigma}{d}$$
$$= \langle\rho\,\boldsymbol{f}\cdot\boldsymbol{n}\rangle\quad\text{on}\quad\Sigma. \tag{25}$$

This equation also reads with

$$\boldsymbol{K}_\Sigma^{-1}\ :=\ \boldsymbol{M}_\Sigma = \begin{pmatrix}M_\tau & M_{\tau n}\\ M_{n\tau} & M_n\end{pmatrix},$$
$$[\![p]\!]_\Sigma = -\mu\,d(M_{n\tau}\,\overline{\boldsymbol{v}\cdot\boldsymbol{\tau}}_\Sigma + M_n\,\overline{\boldsymbol{v}\cdot\boldsymbol{n}}_\Sigma)$$
$$+\mu\left[\!\!\left[\frac{1}{\phi}\,\partial_n(\boldsymbol{v}\cdot\boldsymbol{n})\right]\!\!\right]_\Sigma + d\langle\rho\,\boldsymbol{f}\cdot\boldsymbol{n}\rangle.$$

It is interesting to observe that the mean velocity across Σ satisfies an equation of Brinkman's type with a constant transverse gradient of pressure. Let us point out that, to our knowledge, Eq. (25) is new.

For instance, in the case of a diagonal permeability tensor $\boldsymbol{K}(\phi,\nabla\phi)$ in $\Omega_{\rm fp}$ and using $\overline{\boldsymbol{v}\cdot\boldsymbol{n}}_\Sigma = \boldsymbol{v}\cdot\boldsymbol{n}_{|\Sigma}$, Eq. (25) degenerates to the following transverse Darcy's law if the viscous term can be considered as negligible:

$$\boldsymbol{v}\cdot\boldsymbol{n}_{|\Sigma} = -\frac{\langle K_n(\phi,\nabla\phi)\rangle^h}{\mu}\left(\frac{[\![p]\!]_\Sigma}{d} - \langle\rho\,\boldsymbol{f}\cdot\boldsymbol{n}\rangle\right)\ \text{on}\quad\Sigma, \tag{26}$$

when

$$\left[\!\!\left[\frac{1}{\phi}\,\partial_n(\boldsymbol{v}\cdot\boldsymbol{n})\right]\!\!\right]_\Sigma \approx 0.$$

Equation (26) generalizes the pressure jump below derived by Kubik and Cieszko [74]:

$$[\![p]\!]_\Sigma = -\alpha_0\,\frac{\mu}{\sqrt{K^p}}\,\boldsymbol{v}\cdot\boldsymbol{n}_{|\Sigma},$$

with α_0 a positive dimensionless coefficient.

In particular, for the 1D channel shear flow, i.e., with $\boldsymbol{v}\cdot\boldsymbol{n}=0$ and $\boldsymbol{f}\cdot\boldsymbol{n}=0$, Eq. (26) or (25) with a diagonal permeability tensor $\boldsymbol{K}(\phi,\nabla\phi)$ shows that $[\![p]\!]_\Sigma=0$ and the pressure field is continuous through the interface Σ. This result validates an assumption that is generally admitted by most authors [22–24]. However, $[\![p]\!]_\Sigma$ can be nonzero but possibly weak, if $\boldsymbol{K}(\phi,\nabla\phi)$ is not diagonal even for the 1D flow, and satisfies from Eq. (25)

$$[\![p]\!]_\Sigma=-\mu\, d\, M_{n\tau}\, \overline{\boldsymbol{v}\cdot\boldsymbol{\tau}}_\Sigma.$$

Hence, the multidimensional flow *a priori* involves a nonzero jump of the pressure field across the interface as soon as there is a non-zero transverse flow at the interface. Moreover, by combining Eq. (23) with Eq. (17), we get the normal component of the mean viscous stress vector by

$$\overline{\boldsymbol{\sigma}(\boldsymbol{v},p)\cdot\boldsymbol{n}}_\Sigma\cdot\boldsymbol{n}+\overline{p}_\Sigma=0 \quad \text{on } \Sigma. \tag{27}$$

This links the mean normal stress with the mean pressure on Σ, the pressure jump verifying the transverse Brinkman's Eq. (25) or Darcy's Eq. (26) with $\overline{\boldsymbol{v}\cdot\boldsymbol{n}}_\Sigma=\boldsymbol{v}\cdot\boldsymbol{n}_{|\Sigma}$.

C. Jump interface conditions for a scalar potential and normal flux

Let us now consider the convection-diffusion-reaction problem governing, for example, the heat or mass transfer inside Ω, the scalar potential θ being either the temperature or the mass concentration of a solute transport [13,77,78]:

$$-\nabla\cdot(\boldsymbol{A}\cdot\nabla\theta)+\boldsymbol{v}\cdot\nabla\theta=f \quad \text{in } \Omega, \tag{28}$$

with

$$\boldsymbol{\varphi}(\theta):=-\boldsymbol{A}\cdot\nabla\theta+\boldsymbol{v}\,\theta \text{ and } \boldsymbol{A}:=\begin{pmatrix} A_\tau & A_{\tau n}\\ A_{n\tau} & A_n\end{pmatrix}, \tag{29}$$

where $\boldsymbol{\varphi}(\theta)$ and $\boldsymbol{A}$ are the advection-diffusion flux vector and an symmetric positive definite diffusion tensor, respectively. Furthermore, the volumic source term f can be linear or not like, for example, a reaction term. The effective diffusivity tensor $\boldsymbol{A}_{|\Omega_{fp}\cup\Omega_p}$ inside the porous medium may potentially include a dispersion part. These equations are supplemented by adequate boundary conditions on the external frontier $\Gamma:=\partial\Omega$ supposed to be partitioned in two parts as $\Gamma=\Gamma_D\cup\Gamma_N$. For example, we usually impose the following Dirichlet condition on Γ_D and Fourier-Neumann condition on Γ_N, $\boldsymbol{\nu}$ being the external unit normal vector on Γ_N:

$$\theta=\theta_D \quad \text{on } \Gamma_D,$$
$$\boldsymbol{\varphi}(\theta)\cdot\boldsymbol{\nu}_{|\Gamma_N}=\gamma\,\theta+g \quad \text{on } \Gamma_N, \quad \text{with } \gamma\geqslant 0. \tag{30}$$

By integrating in two different ways the normal flux $\boldsymbol{\varphi}(\theta)\cdot\boldsymbol{n}$ over the thickness of Ω_{fp}, we get with Eq. (28) using the trapezoidal quadrature rule from Lemma 3 and the approximation of the generalized average (iii) from Lemma 4

$$\begin{aligned}\int_{-d/2}^{d/2}\boldsymbol{\varphi}(\theta)\cdot\boldsymbol{n}\,dz &:= -\int_{-d/2}^{d/2}A_{n\tau}\,\nabla_\tau\theta\,dz\\ &\quad -\int_{-d/2}^{d/2}A_n\,\nabla_n\theta\,dz+\int_{-d/2}^{d/2}\boldsymbol{v}\cdot\boldsymbol{n}\,\theta\,dz\\ &\approx d\,\overline{\boldsymbol{\varphi}(\theta)\cdot\boldsymbol{n}}_\Sigma\\ &\approx -d\,\langle A_{n\tau}\rangle^h\,\nabla_\tau\overline{\theta}_\Sigma\\ &\quad -\langle A_n\rangle^h\,[\![\theta]\!]_\Sigma+d\,\overline{\boldsymbol{v}\cdot\boldsymbol{n}}_\Sigma\,\overline{\theta}_\Sigma.\end{aligned}$$

Indeed, the advection velocity $\boldsymbol{v}\cdot\boldsymbol{n}$ in the last term, which can be positive or negative, is first written using the decomposition of any real quantity within the positive and negative part as

$$\boldsymbol{v}\cdot\boldsymbol{n}=(\boldsymbol{v}\cdot\boldsymbol{n})^+-(\boldsymbol{v}\cdot\boldsymbol{n})^-,$$

with

$$(\boldsymbol{v}\cdot\boldsymbol{n})^+:=\max(\boldsymbol{v}\cdot\boldsymbol{n},0)\geqslant 0,$$

$$(\boldsymbol{v}\cdot\boldsymbol{n})^-:=\max(-\boldsymbol{v}\cdot\boldsymbol{n},0)=(-\boldsymbol{v}\cdot\boldsymbol{n})^+.$$

Then, with the positive quantities $(\boldsymbol{v}\cdot\boldsymbol{n})^+,(\boldsymbol{v}\cdot\boldsymbol{n})-\geqslant 0$, we can apply (ii) in Lemma 4 for the two parts and we have using also the trapezoidal rule:

$$\begin{aligned}\int_{-d/2}^{d/2}\boldsymbol{v}\cdot\boldsymbol{n}\,\theta\,dz &= \int_{-d/2}^{d/2}(\boldsymbol{v}\cdot\boldsymbol{n})^+\,\theta\,dz-\int_{-d/2}^{d/2}(\boldsymbol{v}\cdot\boldsymbol{n})^-\,\theta\,dz\\ &\approx d\,\overline{(\boldsymbol{v}\cdot\boldsymbol{n})^+}_\Sigma\,\overline{\theta}_\Sigma-d\,\overline{(\boldsymbol{v}\cdot\boldsymbol{n})^-}_\Sigma\,\overline{\theta}_\Sigma\\ &\approx d\,\overline{(\boldsymbol{v}\cdot\boldsymbol{n})^+-(\boldsymbol{v}\cdot\boldsymbol{n})-}_\Sigma\,\overline{\theta}_\Sigma=d\,\overline{\boldsymbol{v}\cdot\boldsymbol{n}}_\Sigma\,\overline{\theta}_\Sigma.\end{aligned}$$

Since now $|d\,\langle A_{n\tau}\rangle^h\,\nabla_\tau\overline{\theta}_\Sigma|=O(A\,\Theta\,d/L)$, Θ being a reference value of the scalar potential θ, this tangential differential term can be neglected at the order of $O(d/L)$ with respect to the other terms in $O(A\,\Theta)$ or $O(\Theta\,V\,d)$. Thus, we obtain the following equality up to $O(d/L)$:

$$\overline{\boldsymbol{\varphi}(\theta)\cdot\boldsymbol{n}}_\Sigma=-\langle A_n\rangle^h\,\frac{[\![\theta]\!]_\Sigma}{d}+\overline{\boldsymbol{v}\cdot\boldsymbol{n}}_\Sigma\,\overline{\theta}_\Sigma \quad \text{on } \Sigma. \tag{31}$$

Let us notice that the mean normal flux of diffusion on Σ satisfies Fourier's law with a constant transverse gradient across Σ.

Now, we similarly integrate Eq. (28) written in the conservative divergential form:

$$\nabla\cdot\boldsymbol{\varphi}(\theta)=f \quad \text{in } \Omega. \tag{32}$$

Still, integrating Eq. (32) with Lemma 3 and Corollary 1, we have using the mass conservation equation $\nabla\cdot v=0$

$$\nabla_\tau\cdot(d\,\overline{\boldsymbol{\varphi}(\theta)\cdot\boldsymbol{\tau}}_\Sigma)+[\![\boldsymbol{\varphi}(\theta)\cdot\boldsymbol{n}]\!]_\Sigma=d\langle f\rangle.$$

By neglecting again the tangential derivative term of order of $O(\Theta\,V\,d/L)$, we get the following equality up to the order $O(d/L)$:

$$[\![\boldsymbol{\varphi}(\theta)\cdot\boldsymbol{n}]\!]_\Sigma=d\langle f\rangle \quad \text{on } \Sigma. \tag{33}$$

From Eq. (33), we find that when there is no heat or mass source, $\langle f\rangle=0$, then there is no flux jump on Σ: $[\![\boldsymbol{\varphi}(\theta)\cdot\boldsymbol{n}]\!]_\Sigma=0$, and the heat flux is given by Eq. (31) with a temperature jump only.

It is interesting to notice that the algebraic jump interface conditions Eqs. (31) and (33) are of the form proposed in Refs. [27,28] for scalar diffusion-reaction problems, i.e., when the fluid velocity vanishes $\boldsymbol{v}=0$. Moreover, the case of advection-diffusion is also numerically studied in Ref. [32]. The submodel with no flux jump, i.e., $[\![\boldsymbol{\varphi}(\theta)\cdot\boldsymbol{n}]\!]_\Sigma=0$, and thus $\overline{\boldsymbol{\varphi}(\theta)\cdot\boldsymbol{n}}_\Sigma=\boldsymbol{\varphi}(\theta)\cdot\boldsymbol{n}_{|\Sigma}$, was previously considered in Ref. [79]. Moreover, it was also proved in these works that this set of conditions on Σ leads to a mathematically well-posed elliptic problem in the whole domain Ω.

D. Asymptotic model with the first-order algebraic jump interface conditions

Here we summarize the first-order asymptotic model derived in the previous sections for the multidimensional viscous fluid flow with coupled heat or mass transfer inside the fluid-porous system; see Fig. 2.

1. Stokes/Darcy-Brinkman asymptotic model for a centered fictive interface

The set of equations corresponds to a Stokes/Darcy-Brinkman transmission problem inside $\Omega_f \cup \Omega_p$, coupled with the advection-diffusion-reaction equation of the passive scalar:

$$\nabla \cdot \boldsymbol{v} = 0, \quad \text{in } \Omega_f \cup \Omega_p, \tag{34}$$

$$-\mu\,\Delta \boldsymbol{v} + \nabla p = \rho\,\boldsymbol{f}, \quad \text{in } \Omega_f, \tag{35}$$

$$-\widetilde{\mu}\,\Delta \boldsymbol{v} + \mu\,\boldsymbol{K}^{-1}\cdot \boldsymbol{v} + \nabla p = \rho\,\boldsymbol{f}, \quad \text{in } \Omega_p, \tag{36}$$

$$-\nabla\cdot(\boldsymbol{A}\cdot\nabla\theta) + \boldsymbol{v}\cdot\nabla\theta = f, \quad \text{in } \Omega_f \cup \Omega_p, \tag{37}$$

and completed by the so-called *first-order algebraic jump interface conditions (AJIC) on the interface* Σ separating now the pure fluid domain Ω_f from the porous domain Ω_p:

$$[\![\boldsymbol{v}\cdot\boldsymbol{n}]\!]_\Sigma = 0, \tag{38}$$

$$-[\![\boldsymbol{\sigma}(\boldsymbol{v},p)\cdot\boldsymbol{n}]\!]_\Sigma + \mu\,d\,\boldsymbol{K}_\Sigma^{-1}\cdot\overline{\boldsymbol{v}}_\Sigma = d\,\langle\rho\,\boldsymbol{f}\rangle, \tag{39}$$

$$\overline{\boldsymbol{\sigma}(\boldsymbol{v},p)\cdot\boldsymbol{n}}_\Sigma + \overline{p}_\Sigma\,\boldsymbol{n} - \frac{\mu}{\phi_\Sigma}\,\frac{[\![\boldsymbol{v}]\!]_\Sigma}{d} = 0, \tag{40}$$

$$[\![\boldsymbol{\varphi}(\theta)\cdot\boldsymbol{n}]\!]_\Sigma = d\,\langle f\rangle, \tag{41}$$

$$\overline{\boldsymbol{\varphi}(\theta)\cdot\boldsymbol{n}}_\Sigma + \langle A_n\rangle^h\,\frac{[\![\theta]\!]_\Sigma}{d} - \overline{\boldsymbol{v}\cdot\boldsymbol{n}}_\Sigma\,\overline{\theta}_\Sigma = 0. \tag{42}$$

For example, the scalar potential θ may denote either the temperature field for heat transfer or the mass concentration of a solute transport. To close the system of Eqs. (34)–(41), suitable boundary conditions on the external border $\Gamma := \Gamma_D \cup \Gamma_N$ of Ω must be added, e.g., Eq. (11) for the fluid flow and Eq. (30) for the heat or mass transfer.

Moreover, the pressure field inside each subdomain Ω_f or Ω_p is the Lagrange multiplier to verify the equality constraint defined by the mass conservation equation $\nabla\cdot\boldsymbol{v} = 0$. We refer to Ref. [71] for an efficient numerical solution of flow problems with divergence constraint by the augmented Lagrangian technique. Since the pressure is only defined up to an additive constant (different for each subdomain), the two constants can be possibly adjusted so that the pressure jump on Σ satisfies Eq. (25).

2. Stokes/Darcy asymptotic model

Finally, the above asymptotic model also holds when the flow in the porous domain Ω_p is supposed to be governed by the Darcy equation, neglecting the viscous Brinkman's correction by letting formally the effective viscosity $\widetilde{\mu}^p := \widetilde{\mu}_{|\Omega_p} = \varepsilon$ tend to zero; see Ref. [35] for the theoretical justification of the passing to the limit when $\varepsilon \to 0^+$. Indeed, we can show that the viscous dissipation energy $\widetilde{\mu}\,\|\nabla\boldsymbol{v}\|^2_{L^2(\Omega_p)}$ inside Ω_p tends to 0 as soon as $\widetilde{\mu} \to 0$. Moreover, Angot *et al.* [80] calculated the boundary layer due to passing from the Brinkman's model to the Darcy model in the porous subdomain in the case of jump embedded transmission conditions by using the so-called WKB asymptotic expansion. Then, the asymptotic expansion is rigorously justified by proving the convergence and uniform error estimates; see Ref. [80].

Then, the Stokes/Darcy asymptotic model is formally obtained by replacing the Darcy-Brinkman equation in Ω_p Eq. (36) by the Darcy one:

$$\mu\,\boldsymbol{K}^{-1}\cdot\boldsymbol{v} + \nabla p = \rho\,\boldsymbol{f} \quad \text{in } \Omega_p. \tag{43}$$

This also assumes to consider, in the jump interface conditions Eqs. (38) and (40), the trace on Σ of the stress vector in the porous domain Ω_p as defined by

$$\boldsymbol{\sigma}(\boldsymbol{v},p)^p\cdot\boldsymbol{n}_{|\Sigma} := -p^p_{|\Sigma}\,\boldsymbol{n} \quad \text{on } \Sigma. \tag{44}$$

3. Asymptotic model for a noncentered fictive interface

If the fictive interface Σ is not supposed to be centered inside the interfacial region Ω_{fp}, its position is given by the dimensionless parameter $\xi := z_\Sigma/d$; see Fig. 2. Then, using now the approximations defined in Sec. III A to derive the algebraic jump interface conditions, it is an easy matter to verify that the new set of interface conditions is exactly the same as in Eqs. (38)–(42), except that all the mean physical variables on Σ of the type $\overline{\psi}_\Sigma$ are to be replaced by the weighted ones $\overline{\psi}^w_\Sigma$ defined by

$$\overline{\psi}^w_\Sigma = \overline{\psi}_\Sigma + \xi\,[\![\psi]\!]_\Sigma, \quad \text{with} \quad -\frac{1}{2} \leqslant \xi := \frac{z_\Sigma}{d} \leqslant \frac{1}{2}. \tag{45}$$

Let us observe that the jump conditions derived by upscaling in Ref. [19] will be recovered in Sec. IV C with the present asymptotic model only in the case of a noncentered fictive interface.

4. First comments on the asymptotic model

The present asymptotic model, Eqs. (34)–(42), is relatively simple since it is not stated upon upscaling methods from the microscopic pore scale to the macroscopic one by multi-scale homogenization [39,81–83] or volume averaging [13,84]. Its derivation already assumes the macroscopic equations and then averages the different kind of transfer in the thin interfacial region to reduce them to suitable jump conditions on a fictive interface. Hence, the asymptotic model suffers from the lack of information at the microscopic scale, and it must be calibrated by correlation with more complete models coming from upscaling methods or with experiments. That will be the subject of Sec. IV. In particular, this model cannot predict the practical values of effective properties at the interface Σ, i.e., porosity, permeability, diffusion coefficients, or slip coefficients, neither the thickness d of the interfacial layer nor the position of the fictive inner interface defined by $\xi := z_\Sigma/d$. Indeed, the parameters d and ξ remain free parameters, although $\xi = 0$ is the most simple and natural choice for the present practical model.

Besides, when the interfacial region Ω_{fp} is likely to represent the viscous boundary layer between the pure fluid and the porous medium, it is well-known that its thickness d is of the order of $O(\sqrt{\|\boldsymbol{K}^p\|})$; see, e.g., Refs. [1,85,86]. In our framework, we have thus $d = O(\sqrt{K^p})$, and we shall state the scaling as

$$d(\phi_\Sigma) = c(\phi_\Sigma)\sqrt{K^p}, \quad (46)$$

where $c(\phi_\Sigma)$ is a dimensionless function.

Then, the flow in the homogeneous porous domain Ω_p can be described by the Darcy's Eq. (43), so neglecting the Brinkman's viscous correction as explained in Sec. III D 2.

However, the present asymptotic modeling has the great advantage to directly derive the general vector form of the jump interface conditions governing the 2D or 3D viscous flow and heat or mass transfer at a fluid-porous interface. Indeed, as shown in the previous sections, the jumps of all scalar or vector physical quantities are inherently included in the asymptotic formulation. Another original feature of our model is that the interface conditions take the form of equations connecting the jump of all physical variables with the arithmetic mean of traces on each side of Σ, as proposed in Refs. [27,28] for scalar elliptic problems or in Refs. [33,34] for the generalization to vector problems.

IV. COMPARISON WITH EXISTING INTERFACE CONDITIONS

Let us now compare the general asymptotic model Eqs. (34)–(42) with existing interface conditions in the literature. The following comparisons give the scaling of the dimensionless function $c(\phi_\Sigma)$ introduced in Eq. (46) and give the scaling of the slip coefficients introduced by Beavers and Joseph $\alpha_{\rm bj}$ and Ochoa-Tapia and Whitaker $\beta_{\rm otw}$.

A. Comparison with Beavers and Joseph [1]

The semiempirical slip condition of the tangential velocity at Σ for a 1D channel shear flow takes the form

$$\partial_n(\boldsymbol{v}^f\cdot\boldsymbol{\tau})_{|\Sigma} = \frac{\alpha_{\rm bj}}{\sqrt{K^p}}(\boldsymbol{v}^f-\boldsymbol{v}^p)_{|\Sigma}\cdot\boldsymbol{\tau} \quad \text{on } \Sigma, \quad (47)$$

where the dimensionless slip coefficient $\alpha_{\rm bj}$ is positive and only depends on the local structure of the interfacial region. Here, the flow in the homogeneous porous medium Ω_p is described by Darcy's law with constant porosity ϕ^p and isotropic permeability coefficient $K^p(\phi^p)$. Very often, Eq. (47) is simplified considering the approximation $|\boldsymbol{v}^p\cdot\boldsymbol{\tau}_{|\Sigma}| \ll |\boldsymbol{v}^f\cdot\boldsymbol{\tau}_{|\Sigma}|$ [16]. This was theoretically proved by homogenization in Refs. [87–89] for the Beavers-Joseph-Saffman condition and in Ref. [90] for the complete Beavers-Joseph condition. A full jump slip velocity was also recently derived by periodic homogenization [73]; see also Refs. [74,91] for previous other derivations. It is worth recalling that Saffman's assumption is generally not satisfied for large porosity and permeability values (e.g., fibrous porous structures) or for thin fluid layer [92]. Other comments or limitations of this slip condition have been formulated [21,23,25,85,86,93–99].

Since in Beavers-Joseph's configuration, the flow in the porous domain is governed by Darcy's law with $\boldsymbol{v}\cdot\boldsymbol{n}_{|\Sigma} = 0$, the tangential component of Eq. (23) takes the form

$$\frac{\mu}{2}\,\partial_n(\boldsymbol{v}^f\cdot\boldsymbol{\tau})_{|\Sigma} = \frac{\mu}{d\,\phi_\Sigma}(\boldsymbol{v}^f-\boldsymbol{v}^p)_{|\Sigma}\cdot\boldsymbol{\tau} \quad \text{on } \Sigma. \quad (48)$$

The comparison with Eq. (47) using the scaling proposed in Eq. (46) for the thickness $d(\phi_\Sigma)$ of the viscous boundary layer in $\Omega_{\rm fp}$ gives for the slip coefficient $\alpha_{\rm bj}$:

$$\alpha_{\rm bj}(\phi_\Sigma) = \frac{2\sqrt{K^p}}{d\,\phi_\Sigma} = \frac{2}{c(\phi_\Sigma)\,\phi_\Sigma}. \quad (49)$$

Since the scaling for $\alpha_{\rm bj}$ has been estimated by Ref. [86],

$$\alpha_{\rm bj}(\phi_\Sigma) = O\left(\sqrt{\frac{\widetilde{\mu}}{\mu}}\right) = O\left(\frac{1}{\sqrt{\phi_\Sigma}}\right), \quad (50)$$

the scaling of the dimensionless function $c(\phi_\Sigma)$ takes the form

$$c(\phi_\Sigma) = O\left(\frac{1}{\sqrt{\phi_\Sigma}}\right), \quad \text{and thus,} \quad d(\phi_\Sigma) = O\left(\sqrt{\frac{K^p}{\phi_\Sigma}}\right). \quad (51)$$

Let us now consider the tangential component of Eq. (19) for a diagonal permeability tensor $\boldsymbol{K}(\phi,\nabla\phi)$. We have for a noncentered interface Σ with $\langle\rho\,\boldsymbol{f}\rangle = 0$ and Darcy's law in Ω_p:

$$\mu\,\partial_n(\boldsymbol{v}^f\cdot\boldsymbol{\tau})_{|\Sigma} = \frac{\mu\,d}{\langle K_\tau(\phi,\nabla\phi)\rangle^h}\left(\overline{\boldsymbol{v}\cdot\boldsymbol{\tau}}_\Sigma + \xi\,[\![\boldsymbol{v}\cdot\boldsymbol{\tau}]\!]_\Sigma\right) \quad \text{on } \Sigma. \quad (52)$$

This equation completes the Beavers-Joseph condition Eq. (48) by including the dependence on the position ξ of the interface.

Moreover, the pressure jump on Σ described by Eq. (26) is another advantageous feature of the present model in the case of a cross-flow through Σ.

B. Comparison with Ochoa-Tapia and Whitaker [17,18]

For the same 1D configuration, Ref. [17] considers the Darcy-Brinkman equation in the porous region and assuming continuity of velocities at the dividing surface ($\boldsymbol{v}^f\cdot\boldsymbol{\tau}_{|\Sigma} = \boldsymbol{v}^p\cdot\boldsymbol{\tau}_{|\Sigma} := \boldsymbol{v}\cdot\boldsymbol{\tau}_{|\Sigma}$), they derive using the volume averaging method [13] a shear stress jump boundary condition on Σ under the form

$$\partial_n(\boldsymbol{v}^f\cdot\boldsymbol{\tau})_{|\Sigma} - \frac{1}{\phi^p}\,\partial_n(\boldsymbol{v}^p\cdot\boldsymbol{\tau})_{|\Sigma} = \frac{\beta_{\rm otw}}{\sqrt{K^p}}\,\boldsymbol{v}\cdot\boldsymbol{\tau}_{|\Sigma} \quad \text{on } \Sigma, \quad (53)$$

where the dimensionless jump coefficient $\beta_{\rm otw}$ depends on the local structure of the interfacial region but also on the location of the dividing surface. This latter dependence shows that $\beta_{\rm otw}$ can be positive or negative [18]. We also refer to Refs. [14,20,21,100,101] for some further analyses and precisions about this condition and to Refs. [102–104] for the coupled heat transfer or Ref. [105] for the inertial effects.

Let us compare the present asymptotic model Eqs. (34)–(42) with the boundary condition Eq. (53) by taking the tangential component of Eq. (19) with the hypothesis $\boldsymbol{v}\cdot\boldsymbol{n}_{|\Sigma} = 0$. In the absence of body force and for a diagonal permeability tensor $\boldsymbol{K}(\phi,\nabla\phi)$, this yields

$$\partial_n(\boldsymbol{v}^f\cdot\boldsymbol{\tau})_{|\Sigma}-\frac{1}{\phi^p}\,\partial_n(\boldsymbol{v}^p\cdot\boldsymbol{\tau})_{|\Sigma}=\frac{d(\phi_\Sigma)}{\langle K_\tau(\phi,\nabla\phi)\rangle^h}\,\boldsymbol{v}\cdot\boldsymbol{\tau}_{|\Sigma}\quad\text{on}\quad\Sigma. \tag{54}$$

The comparison with Eq. (53) leads to

$$\beta_{\text{otw}}(\phi_\Sigma)=d(\phi_\Sigma)\,\frac{\sqrt{K^p}}{\langle K_\tau(\phi,\nabla\phi)\rangle^h}. \tag{55}$$

Let us recall that the thickness $d(\phi_\Sigma)$ of the interfacial transition layer Ω_{fp} (which is surely included inside the viscous boundary layer) verifies Eq. (46):

$$d(\phi_\Sigma)=c(\phi_\Sigma)\sqrt{K^p}. \tag{56}$$

Under these circumstances, considering Eq. (55) and the scaling of $c(\phi_\Sigma)$ from Eq. (51), we get for the slip coefficient β_{otw}:

$$\beta_{\text{otw}}(\phi_\Sigma)=c(\phi_\Sigma)\,\frac{K^p}{\langle K_\tau(\phi,\nabla\phi)\rangle^h}=O\left(\frac{1}{\sqrt{\phi_\Sigma}}\right)\frac{K^p}{\langle K_\tau(\phi,\nabla\phi)\rangle^h}. \tag{57}$$

Hence, another consequence of the present asymptotic model is that the jump coefficients α_{bj} and β_{otw} are of the same order, and considering Eqs. (50), (51), and (57), we have

$$\beta_{\text{otw}}(\phi_\Sigma)=O(\alpha_{\text{bj}}(\phi_\Sigma))=O\left(\frac{1}{\sqrt{\phi_\Sigma}}\right), \tag{58}$$

with

$$\frac{K^p}{\langle K_\tau(\phi,\nabla\phi)\rangle^h}=O(1).$$

C. Comparison with Valdés-Parada *et al.* [19]

The analysis by Valdés-Parada *et al.* [19] is based on the upscaling of momentum transport in the continuity of the previous study by [17] but without assuming continuity of the velocity field at the fictive interface Σ. The authors propose a new methodology to derive jump boundary conditions for both the velocity and shear stresses. The analysis is based on the fact that the difference between the velocity fields from the single-domain and the two-domain approaches is equal to macroscopic deviations whose determination is obtained by solving associated boundary value problems. The first jump condition obtained, written under the form proposed by Beavers and Joseph [1], takes the form

$$\partial_n(\boldsymbol{v}^f\cdot\boldsymbol{\tau})_{|\Sigma}-\eta_{\text{fp}}\,\alpha\,\partial_n(\boldsymbol{v}^p\cdot\boldsymbol{\tau})_{|\Sigma}=\frac{\alpha}{\sqrt{K^p}}\,(\boldsymbol{v}^f-\phi^p\,\vartheta\,\boldsymbol{v}^p)_{|\Sigma}\cdot\boldsymbol{\tau}\quad\text{on}\quad\Sigma, \tag{59}$$

where η_{fp}, $\alpha/\sqrt{K^p}$, and ϑ are three jump coefficients that are defined in terms of macroscopic closure variables. The second jump boundary condition is given by

$$\partial_n(\boldsymbol{v}^p\cdot\boldsymbol{\tau})_{|\Sigma}-\omega\,\partial_n(\boldsymbol{v}^f\cdot\boldsymbol{\tau})_{|\Sigma}=\frac{\phi^p\,\beta}{\sqrt{K^p}}\,(\boldsymbol{v}^p-\beta_{\text{fp}}\,\boldsymbol{v}^f)_{|\Sigma}\cdot\boldsymbol{\tau}\quad\text{on}\quad\Sigma, \tag{60}$$

where the coefficients ω, β, and β_{fp} are defined in terms of integrals of the associated closure variables.

Let us compare the asymptotic model given by Eqs. (19) and (23) with the above jump boundary conditions. In order to be general, this comparison is performed for a noncentered interface Σ and, therefore, weighted averages are considered in the asymptotic model. Let us first start with the tangential component of condition Eq. (23), where in the absence of body forces and for a diagonal permeability tensor $\boldsymbol{K}(\phi,\nabla\phi)$, we obtain

$$\partial_n(\boldsymbol{v}^p\cdot\boldsymbol{\tau})_{|\Sigma}-\phi^p\,\partial_n(\boldsymbol{v}^f\cdot\boldsymbol{\tau})_{|\Sigma}=\frac{\phi^p\,d(\phi_\Sigma)}{\langle K_\tau(\phi,\nabla\phi)\rangle^h}\left(\xi-\frac{1}{2}\right)\left(\boldsymbol{v}^p+\frac{(\xi+\frac{1}{2})}{(\xi-\frac{1}{2})}\boldsymbol{v}^f\right)_{|\Sigma}\cdot\boldsymbol{\tau}. \tag{61}$$

Let us note that Eq. (61) has exactly the same form of the first jump condition Eq. (60) derived by Valdés-Parada *et al.* [19]. The comparison between those two equations leads to the determination of the coefficients present in Eq. (60):

$$\omega=\phi^p,\quad\beta_{\text{fp}}=-\frac{1}{\phi^p}\frac{(\xi+\frac{1}{2})}{(\xi-\frac{1}{2})},$$

$$\beta=-c(\phi_\Sigma)\left(\frac{1}{2}-\xi\right)\sqrt{\frac{K^p}{\langle K_\tau(\phi,\nabla\phi)\rangle^h}}=O\left[\frac{1}{\sqrt{\phi_\Sigma}}\left(\frac{1}{2}-\xi\right)\right].$$

Let us note that the observations made by Valdés-Parada *et al.* [19] are satisfied. Indeed, ω is of order one, β is found to be negative whatever the location of the fictive interface, and β_{fp} is zero for $\xi=-1/2$. For $\xi=1/2$, $\beta_{\text{fp}}\to\infty$, but in that case $\beta=0$ and continuity of stress is satisfied.

If we now consider the tangential component of the second asymptotic condition Eq. (19), we have

$$\partial_n(\boldsymbol{v}^f\cdot\boldsymbol{\tau})_{|\Sigma}-\frac{1}{\phi^p}\frac{(\xi-\frac{1}{2})}{(\xi+\frac{1}{2})}\,\partial_n(\boldsymbol{v}^p\cdot\boldsymbol{\tau})_{|\Sigma}=\frac{1}{\phi_\Sigma\,d(\phi_\Sigma)}\,\frac{1}{(\xi+\frac{1}{2})}\,(\boldsymbol{v}^f-\boldsymbol{v}^p)_{|\Sigma}\cdot\boldsymbol{\tau}. \tag{62}$$

Again, this jump condition is found to be similar to the the jump condition Eq. (59) derived using the averaging method [19]. The comparison leads to the following expressions for the coefficients:

$$\alpha=\frac{1}{c(\phi_\Sigma)\,\phi_\Sigma}\sqrt{\frac{K^p}{\langle K_\tau(\phi,\nabla\phi)\rangle^h}}\,\frac{1}{(\xi+\frac{1}{2})}=O\left(\frac{1}{\sqrt{\phi_\Sigma}}\,\frac{1}{(\xi+\frac{1}{2})}\right),$$

$$\eta_{\text{fp}}=c(\phi_\Sigma)\left(\xi-\frac{1}{2}\right)\sqrt{\frac{\langle K_\tau(\phi,\nabla\phi)\rangle^h}{K^p}}=O\left(\frac{1}{\sqrt{\phi_\Sigma}}\,\frac{1}{(\xi-\frac{1}{2})}\right),\quad\vartheta=\frac{1}{\phi^p}.$$

Following Ref. [19], we observe that α and η_{fp} are found to be of the same order.

The comparisons presented in the above sections illustrate the relevance of the present asymptotic modeling. Contrary to Ref. [19], it is found that jump conditions for multidimensional flow at the dividing surface can easily be obtained. Nevertheless, let us recall that this methodology is based on the *a priori* knowledge of the one-domain description. Therefore, the exact form of the different coefficients involved in the jump conditions require the spatial evolution of the averaged properties (porosity, permeability,...) in the interregion. As previously mentioned, this description, which was out of the scope of the present analysis, has been recently derived by upscaling local conservation equations in the interfacial region [19].

D. Comparison with Angot [33,34] multidimensional asymptotic model

The jump interface conditions Eqs. (31)–(33) for the heat or mass transfer take the general form proposed in Refs. [27,28] for scalar diffusion-reaction elliptic problems, the case with advection being considered in Refs. [31,32].

For the viscous flow problem, the following algebraic JEBC on Σ are proposed in Refs. [33,34] as a natural and multidimensional generalization of scalar problems:

$$\begin{aligned}
[\![\boldsymbol{\sigma}(\boldsymbol{v},p)\cdot\boldsymbol{n}]\!]_\Sigma &= \boldsymbol{M}\,\overline{\boldsymbol{v}}_\Sigma - \boldsymbol{h} \qquad \text{on } \Sigma,\\
\overline{\boldsymbol{\sigma}(\boldsymbol{v},p)\cdot\boldsymbol{n}}_\Sigma &= \boldsymbol{S}\,[\![\boldsymbol{v}]\!]_\Sigma - \boldsymbol{g} \quad \text{on } \Sigma.
\end{aligned} \tag{63}$$

Here, $\boldsymbol{M}$, $\boldsymbol{S}$ are given *transfer matrices* and $\boldsymbol{h}$, $\boldsymbol{g}$ given vector source terms on Σ. To our knowledge, it was the first model introducing the jumps of both the stress and velocity vectors at the interface for multidimensional viscous flows. This model is also mathematically analyzed in Refs. [33,35] and Ref. [80] for fluid-porous viscous flows.

We can notice that the jump interface conditions Eqs. (19)–(23) and (17) of the present asymptotic model Eqs. (34)–(42) can be written under the general vector form Eq. (63), except that the term $\overline{\boldsymbol{\sigma}(\boldsymbol{v},p)\cdot\boldsymbol{n}}_\Sigma$ in the second equation should be replaced by the mean viscous pseudo-stress vector on Σ:

$$\overline{\boldsymbol{\sigma}_v(\boldsymbol{v})\cdot\boldsymbol{n}}_\Sigma := \overline{\boldsymbol{\sigma}(\boldsymbol{v},p)\cdot\boldsymbol{n}}_\Sigma + \overline{p}_\Sigma\,\boldsymbol{n} = \overline{\frac{\mu}{\phi}\,\nabla\boldsymbol{v}\cdot\boldsymbol{n}}_\Sigma. \tag{64}$$

Hence, it does not affect the tangential shear flow, but the present asymptotic model enables us to precise both the mean normal stress across Σ with Eq. (27) and the pressure jump across Σ with Eq. (25). Furthermore, the present jump interface conditions for the flow Eqs. (38)–(42) read under the general vector form

$$\begin{aligned}
[\![\boldsymbol{v}\cdot\boldsymbol{n}]\!]_\Sigma &= 0 \qquad\qquad \text{on } \Sigma,\\
[\![\boldsymbol{\sigma}(\boldsymbol{v},p)\cdot\boldsymbol{n}]\!]_\Sigma &= \boldsymbol{M}\,\overline{\boldsymbol{v}}_\Sigma - \boldsymbol{h} \quad \text{on } \Sigma,\\
\overline{\boldsymbol{\sigma}(\boldsymbol{v},p)\cdot\boldsymbol{n}}_\Sigma + \overline{p}_\Sigma\,\boldsymbol{n} &= \boldsymbol{S}\,[\![\boldsymbol{v}]\!]_\Sigma - \boldsymbol{g} \quad \text{on } \Sigma.
\end{aligned} \tag{65}$$

We also refer to Refs. [34,35] where the calibration of Eq. (63) is performed for the shear flow with respect to either the shear stress jump condition of Refs. [17,18] using Brinkman's law in Ω_p or the shear velocity jump condition of Ref. [1] with Darcy's law in Ω_p. This is precise for the present asymptotic model in Secs. IV B and IV A, respectively. Then, using the general framework Eq. (63) of JEBC and the analysis proposed in Angot [35], it can be proved that the present jump interface conditions lead to well-posed Stokes/Brinkman or Stokes/Darcy coupled problems.

V. CONCLUSION

An asymptotic modeling for the multidimensional viscous fluid flow and convective transfer at a fluid-porous interface has been derived. The integration of conservation equations over the thickness of the nonhomogeneous interfacial layer present in the one-domain description leads to algebraic jump boundary conditions at a fictive dividing interface between the homogeneous fluid and porous regions of the two-domain approach. The asymptotic analysis has been developed by considering that the thickness d of the interfacial transition region Ω_{fp} is very small compared to the length scale L of the system and therefore, the jump conditions are stated up to first-order in $O(d/L)$.

The analysis has been performed for a multidimensional configuration giving rise to original vector jump boundary conditions. This general formulation also yields a specific equation for the pressure jump at the interface. It has been shown that all the jump conditions derived for the usually 1D-shear flow are recovered by taking the tangential component of the asymptotic model. In that case, the comparison between the asymptotic modeling and the different models available in the literature gives explicit expressions of the effective jump coefficients and the associated scaling.

As far as we know, the present model is probably one of the most general models that can be found in the literature for the noninertial incompressible viscous flow at a fluid-porous interface coupled with heat or mass transfer.

APPENDIX A: ON THE TENSOR $\boldsymbol{K}(\phi,\nabla\phi)$

Let us justify that the expression

$$\boldsymbol{K}(\phi,\nabla\phi)^{-1} := \boldsymbol{K}_d^{-1} - \phi^{-3}\|\nabla\phi\|^2\boldsymbol{I}$$

actually defines the invertible tensor $\boldsymbol{K}$.

We have the equality

$$\begin{aligned}
\boldsymbol{K}_d^{-1} - \phi^{-3}\|\nabla\phi\|^2\boldsymbol{I} &= (\boldsymbol{I} - \phi^{-3}\|\nabla\phi\|^2\boldsymbol{K}_d)\boldsymbol{K}_d^{-1}\\
&= (\boldsymbol{I} - \boldsymbol{B})\,\boldsymbol{K}_d^{-1},
\end{aligned} \tag{A1}$$

with $\boldsymbol{B} := \phi^{-3}\|\nabla\phi\|^2\boldsymbol{K}_d$ verifying with $\|\boldsymbol{K}_d\| = O(\ell^2)$

$$\|\boldsymbol{B}\| = \phi^{-3}\|\nabla\phi\|^2\|\boldsymbol{K}_d\| = O\left(\ell^2/L_\phi^2\right) \ll 1,$$

where L_ϕ denotes the characteristic length scale of porosity variations. Since $\|\boldsymbol{B}\| < 1$, we get with Neumann series

$$(\boldsymbol{I} - \boldsymbol{B})^{-1} = \sum_{k=0}^{+\infty}\boldsymbol{B}^k \approx \boldsymbol{I} + \boldsymbol{B}.$$

Then, we obtain

$$\boldsymbol{K}(\phi,\nabla\phi) := \boldsymbol{K}_d\sum_{k=0}^{+\infty}\boldsymbol{B}^k \approx \boldsymbol{K}_d + \phi^{-3}\|\nabla\phi\|^2\boldsymbol{K}_d^2.$$

Moreover, since $\boldsymbol{K}_d$ is symmetric and positive definite [13], $\boldsymbol{K}$ is also a symmetric and positive definite tensor written as

$$\boldsymbol{K}(\phi,\nabla\phi) = \begin{pmatrix} K_\tau & K_{\tau n} \\ K_{n\tau} & K_n \end{pmatrix}.$$

APPENDIX B: APPROXIMATION RESULTS

Here, we gather and detail some results of approximation that are extensively used throughout the paper. The proofs that are not given can be easily made using standard differential calculus and Taylor series expansions with integral residual; see, e.g., Ref. [106].

Lemma 1 (Integral harmonic mean for diffusion). Let us consider the 1D steady diffusion along the z axis of the scalar potential u over the interval $]a,b[$ $(a < b)$ with no source term and u satisfying the Dirichlet boundary conditions $u(a) := u_a$ and $u(b) := u_b$. The diffusion coefficient A is supposed to be spatially variable and denoted by $A := A(z)$.

Then, the Fourier's diffusive flux φ is constant over $]a,b[$ and the effective or equivalent diffusion coefficient A^e to the layer $[a,b]$ is given by the following harmonic integral average and we have with $h := b - a > 0$,

$$A^e := \langle A\rangle^h := \left(\frac{1}{h}\int_a^b \frac{1}{A(z)}\,dz\right)^{-1} = \frac{1}{\left\langle\frac{1}{A}\right\rangle},$$

and

$$\varphi = -\langle A\rangle^h\,\frac{u_b - u_a}{h}, \tag{B1}$$

where $< . >$ denotes the arithmetic integral mean.

Proof. Using the Fourier diffusion law $\varphi = -A\,\nabla u$, the steady 1D diffusion equation reads

$$\frac{d\varphi}{dz}(z) = -\frac{d}{dz}\left(A(z)\,\frac{du}{dz}\right) = 0.$$

Then, the exact solution verifying the Dirichlet boundary conditions reads

$$u(z) = u_a + \frac{u_b - u_a}{\int_a^b \frac{1}{A(z)}\,dz}\int_a^z \frac{ds}{A(s)},$$

thus

$$\varphi = -\frac{u_b - u_a}{\int_a^b \frac{1}{A(z)}\,dz} = -\langle A\rangle^h\,\frac{u_b - u_a}{h}.$$

■

Remark 1 (Harmonic mean versus arithmetic one for diffusion). More generally, using the harmonic average for equivalent diffusion coefficients gives far more accurate results than with the arithmetic one, since the solution is exact in the above case of Lemma 1. Moreover, with finite volume discretization methods, it allows the discrete fluxes to satisfy the local conservativity and consistency properties that are required for the convergence analysis, even when there are jumps of u at the interfaces between the finite volumes; see Ref. [79]. This is not the case with the arithmetic mean of the diffusion coefficients.

Lemma 2 (Gauss rectangle and midpoint quadrature rules). Let $\omega \subset \mathbb{R}^d$ be an open bounded set of $\mathbb{R}^d$ ($d = 1, 2$ or 3 in practice), and let $\psi : \omega \longrightarrow \mathbb{R}$ be a continuously differentiable function, ψ' being its differential.

Then, for all $x_0 \in \omega$, we have the error estimate

$$\left|\psi(x_0) - \frac{1}{\text{meas}(\omega)}\int_\omega \psi(x)\,dx\right| \leqslant \|\psi'\|_\infty\,\text{diam}(\omega).$$

Hence, it yields $\int_\omega \psi(x)\,dx = \psi(x_0)\,\text{meas}(\omega) + O[\text{diam}(\omega)\,\text{meas}(\omega)]$.

If x_0 is the center of ω and $\psi \in \mathcal{C}^2(\omega)$, then the above approximation of the average $< \psi >$ of ψ over ω is of second-order in $O[\text{diam}(\omega)^2]$ and usually called the midpoint quadrature rule.

Proof. The Taylor expansion with integral residual reads for all $x \in \omega$,

$$\psi(x) = \psi(x_0) + \int_0^1 \psi'(x_0 + t(x - x_0)).(x - x_0)\,dt.$$

By integrating over ω, we get

$$\left|\frac{1}{\text{meas}(\omega)}\int_\omega \psi(x)\,dx - \psi(x_0)\right|$$
$$= \frac{1}{\text{meas}(\omega)}\left|\int_\omega\int_0^1 \psi'(x_0 + t(x - x_0)).(x - x_0)\,dt\,dx\right|$$
$$\leqslant \|\psi'\|_\infty \sup_{x,y\in\omega}|x - y| = \|\psi'\|_\infty\,\text{diam}(\omega).$$

■

Lemma 3 (Trapezoidal quadrature rule). Let $\psi : [a,a + h] \longrightarrow \mathbb{R}$ be a twice continuously differentiable function over the closed bounded interval $[a,a + h] \subset \mathbb{R}$ $(h > 0)$. Then, we have

$$\left|\int_a^{a+h} \psi(x)\,dx - h\,\frac{\psi(a) + \psi(a + h)}{2}\right|$$
$$\leqslant \max_{x\in[a,a+h]} |\psi''(x)|\,\frac{h^3}{12}.$$

In fact, the assumption $\psi'' \in L^1(]a,b[)$ is sufficient to get the third-order approximation of the integral by the trapezoidal quadrature rule.

Lemma 4 (Approximation of the generalized average). Let $\psi : [a,b] \longrightarrow \mathbb{R}$ be a continuous function over the closed bounded interval $[a,b] \subset \mathbb{R}$ with $h := b - a > 0$, and let $w : [a,b] \longrightarrow \mathbb{R}$ be a positive function and Lebesgue-integrable, i.e., $w \in L^1(]a,b[)$ and $w \geqslant 0$. Then,

$$(i)\quad \text{there exists } x_0 \in [a,b], \quad \text{such that}$$
$$\int_a^b \psi(x)\,w(x)\,dx = \psi(x_0)\int_a^b w(x)\,dx.$$

Moreover, if $\psi \in \mathcal{C}^1([a,b])$, we have

$$(ii)\quad \int_a^b \psi(x)\,w(x)\,dx = \psi(x_0)\,h\,\langle w\rangle$$
$$= \langle w\rangle\int_a^b \psi(x)\,dx + O(\|\psi'\|_\infty\langle w\rangle h^2)$$
$$= \langle w\rangle\,h\,\frac{\psi(a) + \psi(b)}{2} + O(\|\psi'\|_\infty\langle w\rangle h^2).$$

If $x_0 = (a+b)/2$ and $\psi \in \mathcal{C}^2([a,b])$, then the above approximation of the integral is of third-order in $O(\|\psi''\|_\infty < w > h^3)$.

If we now assume $w \in L^1(]a,b[)$ and not necessarily positive, the approximation from (ii) still holds and we have

$$(iii) \quad \int_a^b \psi(x)\, w(x)\, dx = \langle w\rangle \int_a^b \psi(x)\, dx + O(\|\psi'\|_\infty < |w| > h^2) = \langle w\rangle h\, \frac{\psi(a)+\psi(b)}{2} + O(\|\psi'\|_\infty < |w| > h^2).$$

Proof. Since the function ψ is continuous over the compact set $[a,b]$, ψ is bounded over $[a,b]$, i.e., $\psi \in L^\infty(]a,b[)$, and with $w \in L^1(]a,b[)$, we have $\psi\, w \in L^1(]a,b[)$. Besides, we have for all $x \in [a,b]$

$$m := \min_{x\in[a,b]} |\psi(x)| \leqslant \psi(x) \leqslant M := \max_{x\in[a,b]} |\psi(x)|.$$

Using the positivity of w and the monotonicity of the integral, the following inequalities hold:

$$m \int_a^b w(x)\, dx \leqslant I := \int_a^b \psi(x)\, w(x)\, dx \leqslant M \int_a^b w(x)\, dx.$$

If now $J := \int_a^b w(x)\, dx = 0$ with $w \geqslant 0$, it means that $w = 0$ at least almost everywhere, and thus also $I = 0$; then, (i) is trivially verified. In the other case where $J \neq 0$, we have dividing by $J > 0$

$$m := \min_{x\in[a,b]} |\psi(x)| \leqslant I/J \leqslant M := \max_{x\in[a,b]} |\psi(x)|.$$

Using the lemma of intermediate values for a continuous function, it yields that I/J is an intermediate value of ψ, i.e., there exists $x_0 \in [a,b]$ such that $\psi(x_0) = I/J$, which proves the equality (i).

With the definition of $< w >$, the equality (i) also reads $I = \psi(x_0)\, h \; < w >$. Hence, using the Gauss rectangle quadrature to write $\psi(x_0)$, x_0 being *a priori* unknown, we get from Lemma 2 for a noncentered point x_0 and $\text{meas}(]a,b[) = \text{diam}(]a,b[) = h = b-a$:

$$\int_a^b \psi(x)\, w(x)\, dx = \langle w\rangle \int_a^b \psi(x)\, dx + O(\|\psi'\|_\infty \langle w\rangle h^2),$$

which shows the first equality of (ii). Now, we use the trapezoidal quadrature rule to express the integral of ψ, which yields the last equality of (ii) with Lemma 3.

When $w \in L^1(]a,b[)$ and not necessarily positive, we introduce the positive part w^+ and negative part w^- of w as follows:

$$w^+(x) := \max\,(w(x),0) \geqslant 0,$$
$$w^-(x) := \max\,(-w(x),0) = (-w(x))^+,$$
$$\text{and thus} \quad w = w^+ - w^-, \quad |w| = w^+ + w^-.$$

Hence, $w^+, w^- \in L^1(]a,b[)$ are both positive functions and applying (i) to each part with two points $x_0, x_1 \in [a,b]$ being *a priori* different, and then (ii) to each part, we get

$$\int_a^b \psi(x)\, w(x)\, dx = (\langle w^+\rangle - \langle w^-\rangle) \int_a^b \psi(x)\, dx + O(\|\psi'\|_\infty(\langle w^+\rangle + \langle w^-\rangle)\, h^2) = \langle w\rangle \int_a^b \psi(x)\, dx + O(\|\psi'\|_\infty \langle |w|\rangle h^2) = \langle w\rangle\, h\, \frac{\psi(a)+\psi(b)}{2} + O(\|\psi'\|_\infty \langle |w|\rangle h^2).$$

This shows (iii) and concludes the proof. ∎

Then using Lemma 4, the key practical result that is extensively used in this study reads as follows.

Corollary 1. (Approximation of the generalized average) Let the function $\psi : [-d/2,d/2] \mapsto \mathbb{R}$ be continuously differentiable and the function $w : [-d/2,d/2] \mapsto \mathbb{R}$ be Lebesgue-integrable. Then, we have

$$\int_{-d/2}^{d/2} \psi(x)\, w(x)\, dx = \langle w\rangle \int_{-d/2}^{d/2} \psi(x)\, dx + O(\|\psi'\|_\infty < |w| > d^2) = d\langle w\rangle \frac{\psi(-d/2)+\psi(d/2)}{2} + O(\|\psi'\|_\infty \langle |w|\rangle d^2) = d\langle w\rangle \overline{\psi}_\Sigma + O(\|\psi'\|_\infty \langle |w|\rangle d^2).$$

[1] G. S. Beavers and D. D. Joseph, J. Fluid Mech. **30**, 197 (1967).
[2] S. K. Gupte and S. G. Advani, Exp. Fluids **22**, 408 (1997).
[3] D. F. James and A. M. J. Davis, J. Fluid Mech. **426**, 47 (2001).
[4] M. F. Tachie, D. F. James, and I. G. Currie, J. Fluid Mech. **493**, 319 (2003).
[5] A. Khalili, I. S. Shivakumara, and S. P. Suma, Transp. Porous Media **51**, 1 (2003).
[6] A. Goharzadeh, A. Khalili, and B. B. Jorgensen, Phys. Fluids **17**, 057102 (2005).
[7] M. Agelinchaab, M. F. Tachie, and D. W. Ruth, Phys. Fluids **18**, 017105 (2006).
[8] M. R. Morad and A. Khalili, Exp. Fluids **46**, 323 (2009).
[9] W.-P. Breugem and B. J. Boersma, Phys. Fluids **17**, 025103 (2005).
[10] R. Rosenzweig and U. Shavit, Water Resour. Res. **43**, W10402 (2007).
[11] F. Liu, B. Cheng, and L. Wang, Exp. Therm. Fluid Sci. **44**, 431 (2013).
[12] E. Arquis and J.-P. Caltagirone, C. R. Acad. Sci. Paris Ser. II **299**, 1 (1984).
[13] S. Whitaker, in *The Method of Volume Averaging*, Theory and Applications of Transport in Porous Media, Vol. 13 (Kluwer Academic Publications, Dordrecht, 1999).
[14] F. J. Valdés-Parada, J. Alvarez-Ramírez, B. Goyeau, and J. A. Ochoa-Tapia, Transp. Porous Media **78**, 459 (2009).

[15] P. Angot, Math. Meth. Appl. Sci. **22**, 1395 (1999).
[16] P. G. Saffman, Stud. Appl. Math. **50**, 959 (1971).
[17] J. A. Ochoa-Tapia and S. Whitaker, Int. J. Heat Mass Transf. **38**, 2635 (1995).
[18] J. A. Ochoa-Tapia and S. Whitaker, Int. J. Heat Mass Transf. **38**, 2647 (1995).
[19] F. J. Valdés-Parada, C. G. Aguilar-Madera, J. A. Ochoa-Tapia, and B. Goyeau, Adv. Water Res. **62**, 327 (2013).
[20] M. Chandesris and D. Jamet, Transp. Porous Media **78**, 419 (2009).
[21] B. Goyeau, D. Lhuillier, D. Gobin, and M. G. Velarde, Int. J. Heat Mass Transf. **46**, 4071 (2003).
[22] H. I. Ene and E. Sanchez-Palencia, J. Mec. **14**, 73 (1975).
[23] T. Lévy and E. Sanchez-Palencia, Int. J. Eng. Sci. **13**, 923 (1975).
[24] M. LeBars and M. G. Worster, J. Fluid Mech. **550**, 149 (2006).
[25] U. Thiele, B. Goyeau, and M. G. Velarde, Phys. Fluids **21**, 014103 (2009).
[26] M. R. Zadiq, R. Usha, and S. W. Joo, Chem. Eng. Sci. **65**, 4443 (2010).
[27] P. Angot, C. R. Acad. Sci. Paris I Math. **337**, 425 (2003).
[28] P. Angot, C. R. Acad. Sci. Paris I Math. **341**, 683 (2005).
[29] P. Angot, F. Boyer, and F. Hubert, in *Finite Volumes for Complex Applications IV—Problems & Perspectives*, edited by F. Benkhaldoun, D. Ouazar, and S. Raghay (Hermes Science, Londres, 2005), pp. 249–260.
[30] P. Angot, F. Boyer, and F. Hubert, Math. Model. Numer. Anal. **43**, 239 (2009).
[31] I. Ramière, P. Angot, and M. Belliard, Comput. Methods Appl. Mech. Eng. **196**, 766 (2007).
[32] I. Ramière, P. Angot, and M. Belliard, J. Comput. Phys. **225**, 1347 (2007).
[33] P. Angot, C. R. Math. Acad. Sci. Paris I **348**, 697 (2010).
[34] P. Angot, in *8th International Conference on Numerical Analysis and Applied Mathematics*, No. AIP-CP 1281 (AIP, New York, 2010), pp. 2208–2211.
[35] P. Angot, Appl. Math. Lett. **24**, 803 (2011).
[36] For the sake of clarity, the present asymptotic model is derived hereafter for the 2D flow with coupled heat or mass transfer, although the extension to 3D is quite straigthforward, since all the tangential derivative and curvature terms are neglected.
[37] G. G. Stokes, On the Theories of the Internal Friction of Fluids in Motion, Ph.D. thesis, Cambridge University, Cambridge, UK, 1845.
[38] For ordered porous media, ℓ can be of the same order of magnitude of η.
[39] E. Sanchez-Palencia, in *Nonhomogeneous Media and Vibration Theory*, Lecture Notes in Physics, Vol. 127 (Springer-Verlag, Berlin, 1980).
[40] E. Sanchez-Palencia, Int. J. Eng. Sci. **20**, 1291 (1982).
[41] T. Lévy, Int. J. Eng. Sci. **21**, 11 (1983).
[42] T. Lévy and E. Sanchez-Palencia, J. Non-Newtonian Fluid Mech. **13**, 63 (1983).
[43] T. Lévy and E. Sanchez-Palencia, Nonlinear Anal. Theory Methods Appl. **9**, 1255 (1985).
[44] A. Brillard, Annales Faculté des Sciences de Toulouse **8**, 225 (1986).
[45] G. Allaire, Asymptotic Anal. **2**, 203 (1989).
[46] G. Allaire, Arch. Ration. Mech. Anal. **113**, 209 (1991).
[47] G. Allaire, Arch. Ration. Mech. Anal. **113**, 261 (1991).
[48] J.-L. Auriault, Transp. Porous Media **79**, 215 (2009).
[49] J. Rubinstein, J. Fluid Mech. **170**, 379 (1986).
[50] J. Rubinstein, J. Stat. Phys. **44**, 849 (1986).
[51] S. Whitaker, Transp. Porous Media **1**, 3 (1986).
[52] J. Barrère, O. Gipouloux, and S. Whitaker, Transp. Porous Media **7**, 209 (1992).
[53] S. Whitaker, Transp. Porous Media **25**, 27 (1996).
[54] H. C. Brinkman, Appl. Sci. Res. **A1**, 27 (1947).
[55] H. C. Brinkman, Appl. Sci. Res. **A1**, 81 (1947).
[56] A. Hill and B. Straughan, J. Fluid Mech. **603**, 137 (2008).
[57] H. Darcy, in *Les fontaines publiques de la ville de Dijon* (Victor Dalmont, Paris, 1856).
[58] V. Marchenko and E. Khruslov, Boundary value problems in domain with granular boundary, *Naukova Dumka, Kiev (in Russian)* (1974).
[59] T. Lundgren, J. Fluid Mech. **51**, 273 (1972).
[60] P. M. Adler, Rheol. Acta **17**, 288 (1978).
[61] J. Koplik, H. Levine, and A. Zee, Phys. Fluids **26**, 2864 (1983).
[62] S. Kim and W. B. Russel, J. Fluid Mech. **154**, 269 (1985).
[63] R. E. Larson and J. J. L. Higdon, J. Fluid Mech. **166**, 449 (1986).
[64] R. E. Larson and J. J. L. Higdon, J. Fluid Mech. **178**, 119 (1987).
[65] N. Martys, D. P. Bentz, and E. J. Garboczi, Phys. Fluids **6**, 1434 (1994).
[66] R. C. Givler and S. A. Altobelli, J. Fluid Mech. **258**, 355 (1994).
[67] A. Einstein, Annalen der Physik **324**, 289 (1906), translated in 1956, *Theory of the Brownian Movement* (Dover Publication, New York, NY, 1956).
[68] F. J. Valdés-Parada, B. Goyeau, and J. A. Ochoa-Tapia, Chem. Eng. Sci. **62**, 4025 (2007).
[69] J.-P. Caltagirone, C. R. Acad. Sci. Paris II **318**, 571 (1994).
[70] P. Angot and J.-P. Caltagirone, in *Proceedings 9th International Heat Transfer Conference*, Vol. 5 (Hemisphere Publishing, Whasington, 1990), pp. 219–224.
[71] K. Khadra, P. Angot, S. Parneix, and J.-P. Caltagirone, Int. J. Numer. Meth. Fluids **34**, 651 (2000).
[72] The notation := is used in order to specify that the equality is taken as a definition.
[73] T. Carraro, C. Goll, A. Marciniak-Czochra, and A. Mikelić, Comput. Methods Appl. Mech. Eng. **292**, 195 (2015).
[74] J. Kubik and M. Cieszko, Continuum Mech. Thermodyn. **17**, 351 (2005).
[75] A. Marciniak-Czochra and A. Mikelić, SIAM Multiscale Model. Simul. **10**, 285 (2012).
[76] T. Carraro, C. Goll, A. Marciniak-Czochra, and A. Mikelić, J. Fluid Mech. **732**, 510 (2013).
[77] H. I. Ene and E. Sanchez-Palencia, Int. J. Eng. Sci. **19**, 117 (1981).
[78] H. I. Ene and E. Sanchez-Palencia, Int. J. Eng. Sci. **20**, 623 (1982).
[79] P. Angot, T. Gallouët, and R. Herbin, in *Finite Volumes for Complex Applications II—Problems & Perspectives*, edited by R. Vilsmeier, F. Benkhaldoun, and D. Hänel (Hermes Publishing, Paris, 1999), pp. 215–222.
[80] P. Angot, G. Carbou, and V. Péron, Asymptot. Anal. **96**, 223 (2016).
[81] A. Bensoussan, J.-L. Lions, and G. Papanicolaou, in *Asymptotic Analysis for Periodic Structures* (North-Holland, Amsterdam, 1978).

[82] E. Sanchez-Palencia, in *Asymptotic Analysis II—Surveys and New Trends*, Lecture Notes in Mathematics, Vol. 985, edited by F. Verhulst (Springer-Verlag, Berlin, 1983), pp. 192–214.
[83] E. U. Hornung, in *Homogenization and Porous Media*, Interdisciplinary Applied Mathematics, Vol. 6 (Springer-Verlag, New York, 1997).
[84] C.-M. Marle, Rev. Inst. Fr. Pet. **22**, 1471 (1967).
[85] G. I. Taylor, J. Fluid Mech. **49**, 319 (1971).
[86] G. Neale and W. Nader, Can. J. Chem. Eng. **52**, 475 (1974).
[87] W. Jäger and A. Mikelić, Ann. Scuola Norm. Sup. Pisa **23**, 403 (1996).
[88] W. Jäger and A. Mikelić, SIAM J. Appl. Math. **60**, 1111 (2000).
[89] W. Jäger, A. Mikelić, and N. Neuß, SIAM J. Sci. Stat. Comput. **22**, 2006 (2001).
[90] A. Brillard, J. E. Amrani, and M. E. Jarroudi, Applic. Anal. **92**, 665 (2013).
[91] M. Cieszko and J. Kubik, Transp. Porous Media **34**, 319 (1999).
[92] C. Zaza, Contribution à la résolution numérique d'écoulements à tout nombre de Mach et au couplage fluide-poreux en vue de la simulation d'écoulements diphasiques homogénéisés dans les composants nuclèaires, Ph.D. thesis, Institut de Mathématiques de Marseille, Aix-Marseille Université, 2015.
[93] S. Richardson, J. Fluid Mech. **49**, 327 (1971).
[94] S. M. Ross, Am. Inst. Chem. Eng. J. **29**, 840 (1983).
[95] M. Sahraoui and M. Kaviany, Int. J. Heat Mass Transf. **35**, 927 (1992).
[96] L. Payne and B. Straughan, J. Math. Pures Appl. **77**, 317 (1998).
[97] D. A. Nield, Transp. Porous Media **78**, 537 (2009).
[98] W. Jäger and A. Mikelić, Transp. Porous Media **78**, 489 (2009).
[99] J.-L. Auriault, Transp. Porous Media **83**, 257 (2010).
[100] M. Chandesris and D. Jamet, Int. J. Heat Mass Transf. **49**, 2137 (2006).
[101] D. A. Nield and A. V. Kuznetsov, Transp. Porous Media **78**, 477 (2009).
[102] J. A. Ochoa-Tapia and S. Whitaker, Int. J. Heat Mass Transf. **40**, 2691 (1997).
[103] J. A. Ochoa-Tapia and S. Whitaker, J. Porous Media **1**, 31 (1998).
[104] B. Alazmi and K. Vafai, Int. J. Heat Mass Transf. **44**, 1735 (2001).
[105] J. A. Ochoa-Tapia and S. Whitaker, J. Porous Media **1**, 201 (1998).
[106] W. Rudin, in *Real and Complex Analysis*, 3rd ed. (McGraw-Hill Inc., Singapore, 1986).